**Doctoral Thesis**

# Photochemical generation of OH radical in water-extract of aerosol and aqueous solution of water-soluble gases in the air

**Sonia Naomi Nomi**

**Graduate School of Biosphere Science**
**Hiroshima University**

**March 2012**

**Doctoral Thesis**

# Photochemical generation of OH radical in water-extract of aerosol and aqueous solution of water-soluble gases in the air

**Sonia Naomi Nomi**

**Environmental Management and Dynamics**

**Graduate School of Biosphere Science**

**Hiroshima University**

**March 2012**

# Contents

# Abstract

This thesis focuses on the oxidation capacity of $^\bullet$OH photogenerated in water-extract of aerosol and aqueous solution of water-soluble gases fraction collected at Hiroshima University and in the Seto Inland Sea. The aqueous phase photoreactions involving $^\bullet$OH is known to play important roles in the troposphere by affecting regional and global climate in various atmospheric photochemical processes and determining the fates of some air pollutants. The aqueous solution of water-soluble gases in ambient air may contain various $^\bullet$OH source compounds such as nitric acid ($HNO_3$), HONO, $H_2O_2$, oxalic acid and other water-soluble organic matter. After transferring to the atmospheric aqueous phase these compounds could generate $^\bullet$OH photochemically. Thus, investigation on sources and sinks of $^\bullet$OH generation is the first step to understanding the capacity and strength of $^\bullet$OH formation in atmospheric aqueous phase and to clarify their influences on photochemical reactions occurring in the air.

The overall structure of the thesis includes 4 chapters. *Chapter 1* introduces the basic concepts of the atmospheric aerosol and the photochemical mechanisms of $^\bullet$OH generation occurring in aqueous phase. The role and significance of $^\bullet$OH in the atmosphere and past results obtained by other investigators and the contributions to this field of research are shown.

The following *Chapter 2* reports the collection of ambient aerosol at Higashi-Hiroshima campus using a coupled sampler for simultaneous collection of both phases, water-extracts of aerosols (WEA) and aqueous solution of water-soluble gas fraction (WSG) during June/2008 to June 2010. The $^\bullet$OH photoformation rate ($R_{OH}$) and chemical composition of both fractions were determined. Among the major anions present in the WSG and WEA samples, the $SO_4^{2-}$ concentration was highest followed by $NO_3^-$ and $Cl^-$. The mean concentration of $SO_4^{2-}$ was $9.4\pm4.0$ nmol m$^{-3}$ in the WSG and $81\pm33$ nmol.m$^{-3}$ for the WEA. The $R_{OH}$ determined and normalized based on the air-volume, which revealed values of 1.4 and 0.5 nmol h$^{-1}$ m$^{-3}$ for the WEA and WSG, respectively. The contribution of $NO_3^-$, $NO_2^-$ and $H_2O_2$ as the main sources of $^\bullet$OH via photolysis were 4.5, 0.7 and 1.2%, respectively, for the WSG fraction, while in the WEA fraction, $NO_3^-$, $NO_2^-$ and $H_2O_2$ contributed 8.9, 1.2 and 2.5%, respectively. DOC, which was determined only for WSG samples, ranged from 0.1 to 5.3 mg C m$^{-3}$ with a mean of $2.9\pm2.6$ mg C m$^{-3}$. To find potential sources of $^\bullet$OH in the atmospheric aqueous phase, known amount (excess) of iron (III) was added into the solution of the WSG fraction and then the $R_{OH}$ of photo-Fenton reaction was determined. The photo-Fenton reaction contributed 42% of the total $^\bullet$OH formation in the WSG fraction, while unknown sources that might have been humic-like substances (HULIS) accounted for

the remaining 52%. The results showed high contribution from unknown sources and fluorescent properties very similar to those existing in natural waters and water-extract of aerosol.

*Chapter 3* follows similar methodologies used in the previous chapter, however using a high volume sampler for the sampling, reports the photochemistry of the $^\bullet$OH in water-extract of marine aerosol collected in the Seto Inland Sea during a research cruise in summer of 2010. Unlike the ambient aerosols collected on land, the chemical composition showed large influence of the sea-salt ions such as $Na^+$ and $Cl^-$ and the oxidation capacity of the $^\bullet$OH much lower compared to aerosols collected on land, indicating minor influence of anthropogenic activities on the photochemical generation of $^\bullet$OH. The mean concentration of $Cl^-$ and $Na^+$ were 36.3±51 nmol m$^{-3}$ and 47.7±34 nmol m$^{-3}$ respectively. $Cl^-$ represents 47.6% and $Na^+$ represents 52.6% of the total ions measured. Low percentages of $SO_4^{2-}$ (32.1%) and $NO_3^-$ (20.5%) are good indicators for marine aerosol. $NO_2^-$ was present in only 2 of the total 16 samples (mean of 1.39 nmol m$^{-3}$). The mean concentration of DOC was 7.0±6.6 mg C m$^{-3}$ and the mean pH was 6.18±0.114.

The $^\bullet$OH photoformation rate ranged from 0.019-0.014 with the mean of 0.06±0.03 nmol h$^{-1}$ m$^{-3}$. Among the major sources of $^\bullet$OH, $NO_3^-$ accounted for 18.6% while the

unknown sources contributed for about 74%. The occurrence of unknown sources, possibly HULIS, as the main and important contributor of $^{\bullet}$OH generation in marine aerosol samples. Formation mechanism involving the photolysis of DOM such as HULIS, which have been suggested to be the major source of $^{\bullet}$OH formation in the river and sea waters.

In the *Chapter 4* a general discussion on the obtained results and the suggestion of further research are made. Sources and sinks of $^{\bullet}$OH in the WEA fractions from land and marine aerosols are almost same to those in the WSG fractions. In addition, mechanism of $^{\bullet}$OH generations occurring in atmospheric aqueous phase, in which HULIS is involved, are probably same/identical to those in natural waters. Therefore, in the analogue of photoformed $^{\bullet}$OH in natural waters, $^{\bullet}$OH in the WEA and WSG fractions in the atmosphere may significantly control for the aerosol and gas phase chemistry, especially degradation rates of several organic matter.

論文題目：大気中エアロゾルの水抽出画分およびガスの水溶性画分におけるヒドロキシルラジカルの光化学的生成速度に関する研究

広島大学大学院生物圏科学研究科 **環境循環系制御学** 専攻

Nomi Sonia Naomi

　本研究では、大気中エアロゾル（微細粒子）中で光化学的に生成するヒドロキシルラジカル（OH ラジカル）の生成過程に関して研究を行った。大気試料は、東広島市及び瀬戸内海海上において採取した。大気エアロゾル中の OH ラジカルの主な生成源として、大気気相（ガス）中の水溶性成分が考えられるので、大気気相中の水溶性成分も同時に採取し、比較検討した。

　第 1 章は序論であり、大気エアロゾルの大気汚染、酸性雨、地球温暖化・冷却化に及ぼす作用について紹介し、大気エアロゾル中で OH ラジカルの存在状態や役割に関して考察した後、本研究の意義や目的を述べている。

　第 2 章では、東広島において 2008 年から 2010 年にかけて月 1 回合計 24 回大気試料を採取し、エアロゾルの水抽出画分およびガスの水溶性画分をそれぞれ分離して OH ラジカルの光化学的発生速度を求めた。その結果、大気エアロゾルの水抽出画分およびガス水溶性画分中 OH ラジカルの平均発生速度はそれぞれ 1.4 および 0.5 nmol h$^{-1}$ m$^{-3}$であり、硝酸イオン、亜硝酸イオン、過酸化水素の光分解からの発生寄与率は水抽出画分でそれぞれ 8.9、1.2、2.5%、水溶性画分で 4.5、0.7、1.2%であった。その他成分からの発生寄与率はガス水溶性画分で光フェントン反応から 42%、溶存有機物（おそらく腐植様物質）から 52%であった。OH ラジカルの生成速度の月毎の変動を解析したところ、季節変化は見られないものの、黄砂飛来時にはエアロゾル水抽出画分の OH ラジカルの生成速度が増加する傾向があることが確認された。黄砂時の OH ラジカル生成速度の増加は、黄砂粒子中に含まれる硝酸塩や水溶性有機物の光分解に原因すると推察した。

　第 3 章では、瀬戸内海海上大気中のエアロゾル中 OH ラジカルの生成過程を調べた。2010 年夏の広島大学生物生産学部実習船豊潮丸の瀬戸内海航海において、海上大気中エアロゾルを船首デッキで採取した。エアロゾルの水抽出画分中 OH ラジカルの平均発生速度は 0.06 nmol h$^{-1}$ m$^{-3}$であり、硝酸イオンからの発生寄与率は 19%であった。その他成分からの発生寄与率は 74%であった。また、その他成分は腐植様物質の可能性が高いことが 3 次元蛍光分析から示唆された。

　第 4 章は総合討論、結論、今後の課題を述べている。本研究により、大気エアロゾル中での OH ラジカルの発生過程には硝酸イオンなどの無機物以外に、腐植様物質のような有機物が関与することが示唆された。また、大気ガスの水溶性画分からも OH ラジカルが発生することから、エアロゾル中 OH ラジカルの発生物質の一部は大気ガスから移行してきたものであることが推察された。光化学的に発生した OH ラジカルは、エアロゾル液相中で多くの化学物質の酸化還元反応に関与することで、それらの大気中での寿命や動態を決定すると考えられる。したがって、OH ラジカルの消失過程に関する研究が今後の課題といえる。

# Chapter 1

# Chapter 1

## 1-1-General Introduction

Historically, the field of atmospheric chemistry has focused on gas-phase oxidations as the primary fate-determining processes of chemical substances in the troposphere. However, there is increasing evidence demonstrating that aqueous-phase photochemical transformations in atmospheric water drops (cloud, fog, and rain drops, and aqueous aerosols) can significantly affect the chemical composition of the troposphere (Finlayson-Pitts and Pitts, 2000).

Aerosols, defined as suspensions of solid or liquid particles in a gas, are currently of interest for a number of reasons. Their potential to offset global warming, the optical properties of aerosols mean that they are efficient scatters of light, aerosols have the potential to both heat and cool the surface of the earth (Seinfeld and Pandis, 1998; Finlayson-Pitts and Pitts, 2000; Ramanathan *et al.*, 2001). Aerosol particles present surface area to reactive gaseous species that can provide new pathways for atmospheric chemical reactions and/or serves as sinks for reactive species such as free radicals. Aerosol particles serve as cloud condensation nuclei thereby altering the composition of cloud water and influencing the course of aqueous reactions in clouds. Through scattering and absorption of radiation in the solar spectrum aerosol particles influence the rate of primary photochemical reactions (Heintzenberg *et al.,* 2003). They control the visibility in the air, the intensity of solar radiation reaching the surface of our planet, as well as electric and radioactive properties of the atmospheric environment (Bizjak *et al.*, 1999)

Reactions taking place in the atmosphere are extremely important because they significantly influence the lifetime of many atmospheric components and yield intermediates that often play a key role in atmospheric chemistry (Vione *et al.*, 2006). The

fate of numerous organic and inorganic compounds in the atmosphere is controlled by photochemically produced oxidants (Calvert *et al.*, 1966; Finlayson-Pitts and Pitts, 2000; Warneck, 1988).

The chemical transformations occurring in the atmosphere are best characterized as oxidation processes. Solar radiation influences the chemical processes in the atmosphere by interacting with molecules that act as photo acceptors (Boubel *et al.*, 1973).

Reactive oxygen species (ROS) have been defined according to their own name, to derive and present higher reactivity due of unpaired electrons than molecular oxygen with redox activity (Pardini, 1995; Murrant and Reid, 2001). It includes families of oxygen-centered or related free radicals, ions, and molecules. The free radical family includes superoxide ($^{\bullet}O_2^-$), hydroxyl ($^{\bullet}OH$), hydroperoxyl ($^{\bullet}O_2H$) and organic peroxy radicals. Non-radicals such as hydrogen peroxide ($H_2O_2$), singlet oxygen ($^1O_2$), hypochlorous acid (HOCl) (Fink, 2002) and organic and inorganic peroxides also come under the umbrella of 'Reactive Oxygen Species' (Figure 1).
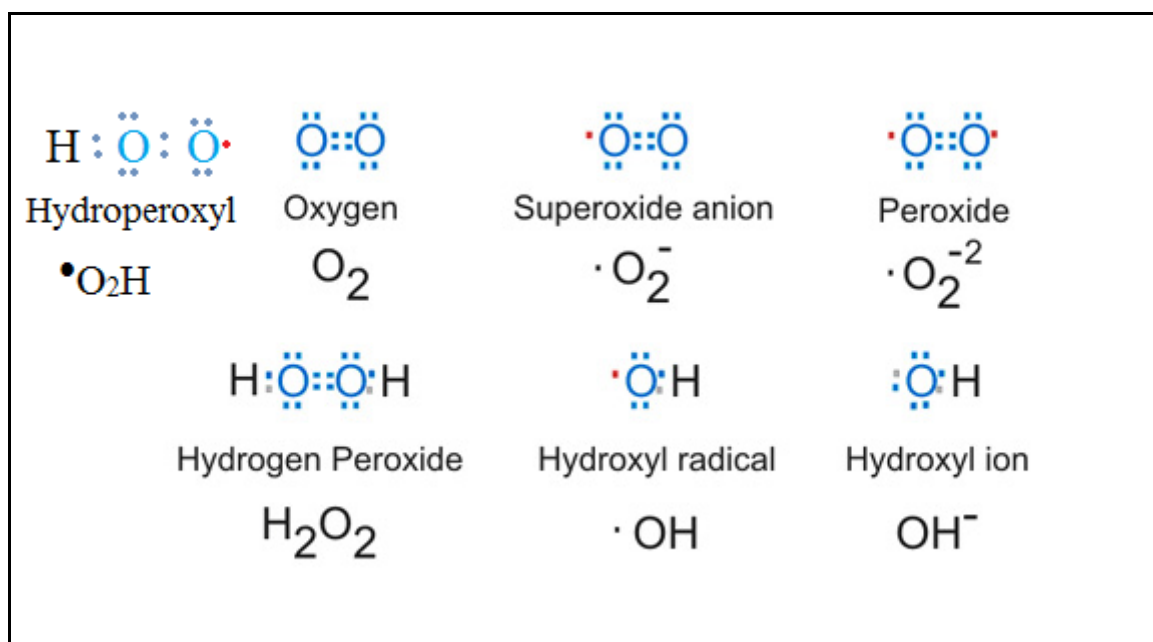


**Figure 1.** Reactive Oxygen Species

**1-2-Atmospheric Hydroxyl Radical**

$^\bullet$OH is the most powerful daytime oxidant among ROS generated as short-lived intermediates in tropospheric chemistry (second-order rate constants of $10^7$ to $10^{10}$ $M^{-1}$ $s^{-1}$). Occurring in aqueous phase at very slow steady-state concentrations, this is difficult to monitor directly by spectroscopy methods (Buxton *et al.*, 1988). Due to its high oxidation potential for the removal of air pollutants, $^\bullet$OH is referred to as the "detergent" or "vacuum cleaner" of the atmosphere (Thompson, 1992). The oxidation capacity of most organic substances has attracted many researchers focus on the role of the $^\bullet$OH as an oxidant in the environment (Zepp *et al.*, 1992).

In the atmospheric gas phase, $^\bullet$OH is generated by photochemical mechanisms such as photolysis of ozone ($O_3$), nitrous acid (HONO), hydrogen peroxide ($H_2O_2$), methyl-hydroperoxide ($CH_3OOH$), and carbonyl compounds (mainly aldehydes and ketones) (Atkinson, 2000; Moortgat, 2001).

In the atmospheric aqueous phase, $^\bullet$OH is generated by the photolysis of nitrate ions ($NO_3^-$) (reaction 1), nitrite ions ($NO_2^-$/$HNO_2$) (reactions 2 and 3) and hydrogen peroxide ($H_2O_2$) (reaction 4). Moreover, in the Fenton reaction, $^\bullet$OH is produced by the reaction between reduced iron, $Fe^{2+}$, and $H_2O_2$ (reaction 5) (Zellner *et al.* 1990). Iron (III), which may exist in the form of complexes with natural dissolved organic matter (DOM) such as oxalic acid and humic-like substances (HULIS) in the aqueous phase, is photochemically reduced to $Fe^{2+}$ through a ligand-to-metal charge transfer. The $Fe^{2+}$ subsequently reacts with $H_2O_2$ (reactions 6 to 8) (Voelker *et al.* 1997). Furthermore, direct photolysis reactions of DOM such as p-benzoquinone and HULIS may act as sources of $^\bullet$OH in the atmospheric aqueous phase, through mechanisms similar to those that occur in natural water chemistry

(Alegría *et al.* 1997; Vaughan and Blough, 1998). However, the generation mechanisms of $^\bullet$OH have not been fully characterized to date.

$$NO_3^- + H_2O + h\nu \rightarrow \ ^\bullet OH + OH^- + NO_2 \qquad\qquad (1)$$

$$NO_2^- + H_2O + h\nu \rightarrow \ ^\bullet OH + OH^- + NO \qquad\qquad (2)$$

$$HONO + h\nu \rightarrow \ ^\bullet OH + NO \qquad\qquad (3)$$

$$H_2O_2 + h\nu \rightarrow 2 \ ^\bullet OH \qquad\qquad (4)$$

$$Fe^{2+} + H_2O_2 + H^+ \rightarrow Fe^{3+} + \ ^\bullet OH + H_2O \qquad\qquad (5)$$

$$Fe^{3+} + C_2O_4^{2-} \rightarrow [Fe^{3+} (C_2O_4)]^+ \qquad\qquad (6)$$

$$[Fe^{3+} (C_2O_4)]^+ + h\nu \rightarrow [Fe^{2+} (C_2O_4)]^+ \qquad\qquad (7)$$

$$[Fe^{2+} (C_2O_4)]^+ + O_2 \rightarrow Fe^{2+} + O_2^- + 2CO_2 \qquad\qquad (8)$$
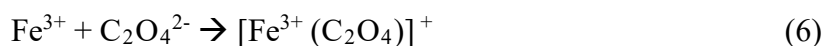
Even though studies of $^\bullet$OH photoformation in cloud droplets, fog, dew and rain have been conducted (Faust and Allen, 1993; Faust *et al.*, 1993; Arakaki and Faust, 1998, Arakaki *et al.*, 1998, Anastasio *et al.*, 1994; Nakatani *et al.*, 2007), only a few studies have investigated the water-extract of atmospheric aerosols (Arakaki *et al.*, 2006, Kondo *et al.*, 2009); therefore, sources and sinks of $^\bullet$OH have not been clarified.

Moreover, no studies that have been conducted to date have focused on photoformation of $^\bullet$OH in aqueous solutions of water-soluble gases in the atmosphere, even though an understanding of this process may be useful for evaluation of the oxidation capacities of ambient air. Therefore, this study was conducted to determine the $^\bullet$OH photoformation rate, as well as its sources and contributions in both the water-extract of aerosol and aqueous solution of water-soluble gas in air samples.

### 1-3-Outlines of this study

The overall structure of the thesis includes 4 chapters. It consists of two main parts: first part is about the study of the $^{\bullet}OH$ generation capacity in the water-extracts of aerosols (WEA) and aqueous solution of water-soluble gas (WSG) fractions collected at Hiroshima University. Chemical composition, the main sources and source strengths of $^{\bullet}OH$ generation in ambient aerosol and aqueous soluble gases were investigated (*Chapter 2*). The air sampling system used for the collection of both gas and particle fractions was set up to collect relatively low-volume air samples.

The second part deals with water-extracts of marine aerosols collected from the Seto Inland Sea region using a high-volume air sampler for determination of the oxidative capacity of $^{\bullet}OH$ (*Chapter 3*).

The research concerns of this thesis are:

1) To acquire information about the oxidation capacity of $^{\bullet}OH$ in the water-extracts of aerosols and aqueous solution of water-soluble gas fractions in atmospheric ambient land air (*Chapter 2*).

2) To identify the main sources, source intensities and mechanisms for the $^{\bullet}OH$ formation of the ambient air of Higashi-Hiroshima, Japan (*Chapter 2*).

3) To determine the $^{\bullet}OH$ formation rate ($R_{OH}$), the chemical composition and contribution from the major sources of $^{\bullet}OH$ in water-extracts of marine aerosols collected from the Seto Inland Sea region, in western Japan (*Chapter 3*).

# References

Alegría, A.E., Ferrer, A. and Sepúlveda, E., 1997. Photochemistry of water-soluble quinones. Production of water-derived spin adduct. Photochemistry and Photobiology 66(4), 436-442.

Anastasio, C., Faust, B.C., and Allen, J.M., 1994. Aqueous phase photochemical formation of hydrogen peroxide in authentic cloud waters. Journal of Geophysical Research 99 (D4), 8231-8248.

Arakaki, T., Miyake, T., Shibata, M. and Sakugawa, H., 1998. Measurement of photochemically formed hydroxyl radical in rain and dew waters. The Chemical Society of Japan, 9, 619-625 (in Japanese).

Arakaki, T. and Faust, B.C., 1998. Sources, sinks, and mechanisms of hydroxyl radical (OH) photoproduction and consumption in authentic acidic continental cloud waters from Whiteface in Mountain, New York: the role of the Fe(r) (r = II, III) photochemical cycle. Journal of Geophysical Research 103 (D3), 3487-3504.

Arakaki, T., Kuroki, Y., Okada, K., Nakama, Y., Ikota, H., Kinjo, M., Higuchi, T., Uehara, M.; Tanahara, A., 2006. Chemical composition and photochemical formation of hydroxyl radicals in aqueous extracts of aerosol particles collected in Okinawa, Japan. Atmospheric Environment 40, 4767-4774.

Atkinson, R., 2000. Atmospheric chemistry of VOCs and $NO_x$. Atmospheric Environment 34, 2063-2101.

Bizjak, M., Grgié, Hudnik, V., 1999. The role of aerosol composition in the chemical processes in the atmosphere. Chemosphere, Vol. 38, no. 6, 1233-1240.

Boubel, R.W., Fox, D.L., Turner, D.B., and Stern, A.C., 1973. Fundamentals of air pollution, 3$^{rd}$ edition – Academic Press USA, page 165.

Buxton, G. V., Greenstok, C. L., Helman, W.P., Ross, A. B., 1988. Critical review of rate constants for reactions of hydrated electron, hydrogen atoms and hydroxyl radicals (OH/O$^-$) in aqueous solution. Journal of Physical Chemistry. Ref. Data 17, 513.

Calvert, J.G., Pitts, J.N. Jr, 1966. Photochemistry. Wiley, New York, 899.

Faust, B.C. and Allen, J.M., 1993. Aqueous-phase photochemical formation of hydroxyl radical in authentic cloudwaters and fogwaters. Environmental Science and Technology 27, 1221-1224.

Faust, B.C., Anastasio, C., Allen, J.M., Arakaki, T., 1993. Aqueous-phase photochemical formation of peroxides in authentic cloud and fog waters. Science 260, 73-75.

Fink, M.P., 2002. Role of reactive oxygen and nitrogen species in acute respiratory distress syndrome. Curr Opin Crit Care, 8:6–11.

Finlayson-Pitts, B. J. and Pitts, J. N. J., 2000. Chemistry of the Upper and Lower Atmosphere, Academic Press, San Diego, California.

Heintzenberg, J., Raes, F., Schwartz, S. E., 2003. Atmospheric Chemistry in a Changing World – an Integration and Synthesis of a Decade of Tropospheric Chemistry Research. Eds., Springer, Berlin, pp. 125-156. (Chapter 4 available online)

Kondo, H., Chiwa, M., Sakugawa, H., 2009. Photochemical formation and scavenging mechanisms of hydroxyl radical in water-extracts of atmospheric aerosol collected in Higashi-Hiroshima, Japan. Geochemical Chemistry 43, 15-25 (in Japanese)

Moortgat, G.K., 2001. Important photochemical processes in the atmosphere. Pure and Applied Chemistry, 73 (3), 487-490.

Murrant, C.L. and Reid, M.B., 2001. Detection of reactive oxygen and reactive nitrogen species in skeletal muscle. Microscopy Research and Technique, 55:236– 48.

Nakatani, N., Ueda, M., Shindo, H., Takeda, K., and Sakugawa, H., 2007. Contribution of the Photo-Fenton reaction to hydroxyl radical formation rates in river and rain water samples. Analytical Sciences, 23, 1137-1142.

Pardini, R.S., 1995. Toxicity of oxygen from naturally occurring redox-active pro-oxidants. Arch Insect Biochem Physiol, 29:101–18.

Ramanathan, V. *et al.*, 2001. Indian Ocean Experiment: An integrated analysis of the climate forcing and effects of the great Indo-Asian haze. Journal of Geophysical Research 106: 28371–28399, doi: 10.1029/2001JD900133.

Seinfeld, J.H. and Pandis, S.N., 1998. Atmospheric Chemistry and Physics: From Air pollution to climate Change. 1$^{st}$ edition, J. Wiley, New York.

Thompson, A.M., 1992. The oxidizing capacity of the earth's atmosphere: Probable past and future changes. Science 256, 1157-1165.

Vaughan, P.P. and Blough, N.V., 1998. Photochemical formation of hydroxyl radical by constituents of natural waters. Environmental Science and Technology 32, 2947-2953.

Vione, D., Maurino, V., Minero, C., Pelizzetti, E., Harrison, M.A.J., Olariu, R., and Arsene, C., 2006. Photochemical reactions in the tropospheric aqueous phase and on particulate matter. Chemical Society Review, 35, 441-453.

Voelker, B.M., Morel, F.M.M. and Sulzberger, B., 1997. Iron redox cycling in surface waters: Effects of humic substances and light. Environmental Science and Technology 31, 1004-1011.

Warneck, P., 1988. Chemistry of the Natural Atmosphere 41, Academic press: San Diego International Geophysics Series.

Zellner, R., Exner, M. and Herrmann, H., 1990. Absolute OH quantum yields in the laser photolysis of nitrate and dissolved $H_2O_2$ at 308 and 351 nm in the temperature range 278-353 K. Journal of Atmospheric Chemistry, 10, 411-425.

Zepp, R.G.; Faust, B.C. and Hoigné, J., 1992. Hydroxyl radical formation in aqueous reactions (pH 3-8) in iron (II) with hydrogen peroxide: The photo-Fenton reaction. Environmental Science and Technology 26, 313-319.

# Chapter 2

**Chapter 2**

**Photoformation of OH radical in water-extracts of atmospheric aerosols and aqueous solution of water-soluble gases collected in Higashi-Hiroshima, Japan**

**2-1-Introduction**

It is widely accepted that hydroxyl radicals ($^\bullet$OH) play an important role in the oxidation of various organic and inorganic compounds in not only atmospheric gas phase but also atmospheric aqueous systems (i.e. aerosols, cloud fog, dew and rain) (Finlayson-Pitts and Pitts, 1986). $^\bullet$OH is the most powerful daytime oxidant among reactive oxygen species (ROS) generated as short-lived intermediates in tropospheric chemistry (Finlayson-Pitts and Pitts, 1986). $^\bullet$OH can be formed via photochemical reactions in sunlight-illuminated aqueous phase through a variety of mechanisms as previously detailed in the *Chapter 1*.

Even though studies of $^\bullet$OH photoformation in cloud droplets, fog, dew and rain have been reported (Faust *et al*., 1993; Arakaki and Faust, 1998, Arakaki *et al*., 1998, Anastasio *et al*., 1994), only a few studies were made for water extract of atmospheric aerosol particles (Arakaki, *et al*., 2006, Kondo *et al*., 2009), and thus sources and sink of $^\bullet$OH are still not yet clarified. Moreover no studies to date have focused on photoformation of $^\bullet$OH in the water-soluble gaseous fraction of the atmosphere, which may be useful for evaluation of oxidation capacities of ambient air.

Therefore, this study was conducted to determine the $^\bullet$OH photoformation rate, its sources and contribution in both the water-extract of aerosol and water-soluble gaseous fractions of ambient air samples collected in Higashi-Hiroshima.

## 2-2- Experimental

### 2-2-1- Sampling site

Higashihiroshima is a university town of Hiroshima University. As the central city of Hiroshima Central Technopolis, high-tech industry is growing. Higashihiroshima is adjacent to Hiroshima city, so it is also a commuter town of Hiroshima. Atmospheric aerosol particle and gas fraction samples were collected monthly on the roof of the Faculty of Integrated Arts and Sciences building of Hiroshima University (about 30 m above ground level) at the Higashi-Hiroshima campus (34°24'N, 132°42'E, altitude 242 meters) (Figure 2-1), Japan, from June 2008 to June 2010 (n= 24). As of June 2011, Higashi-Hiroshima had an estimated population of 183,834 in a total area of 635, 32 km².

### 2-2-2- Reagents

All chemicals and solvents were of reagent grade and were used as received without further treatment. All reagent solutions were prepared using ultrapure water (Milli-Q, $\geq 18$ M$\Omega$ cm, Millipore Japan).

### 2-2-3- Air sampling

An air filtering unit combined with two sequential scrubber vessels (impingers) was used to collect samples (Figure 2-2). A silica fiber filter (QR-100, $\phi$= 47 mm, 0.3 $\mu$m pore size) was attached to the system input to collect aerosol particles. The collection system was also connected to two sequential gas scrubbers containing 500 ml of Milli-Q water as an absorption solution for collection of atmospheric aqueous solution of water-soluble gas (WSG). The flow rate was maintained at 1.5-2.0 L min$^{-1}$ using an air pump (AP-032Z Model, Iwaki Air Pump APN-215 NV-1) for approximately 2-7 days, during which time 8.3 to 29 m$^3$ of ambient air were collected.

A blank control filter was analyzed in the same manner as the aerosol filters, after being kept in a clean room for one week without being connected to the pump. Additionally, Milli-Q water (500 ml) was kept in the impinger for one week and used as a blank control solution for the WSG fraction. The Milli-Q water was analyzed for inorganic ions and metal species to check for possible contamination from the impinger and other instruments in the collection device and, if found contaminants were found, the WSG fraction was corrected (Figure 2-3).

The aerosol collected on the fiber filters and the blank control filter were stored in polyethylene plastic bags and the absorption solutions were stored in polyethylene plastic bottles under refrigeration until further extraction and analytical measurements were conducted.

## 2-2-4- Extraction procedure and analytical methods

The sampled aerosol filter (WEA fraction) was soaked in 20 mL of Milli-Q water for three hours shaking at 120 rpm using a multishaker (MMS-310, EYELA). The sample was then filtered using a syringe filter with a 0.45 µm pore size (Pall, Akrodisc 25mm) before being subjected to photochemical experiments and chemical analyses.

## 2-2-5- Chemical analysis of water-soluble fractions

The concentrations of the major inorganic ions, dissolved organic carbon (DOC) and $H_2O_2$ were measured using ion chromatography (ICS –1600, Dionex), a TOC analyzer (TOC-5000A, Shimadzu) and isocratic HPLC (LC-10Ai, Shimadzu), respectively. The total dissolved iron and other heavy metals were determined using inductively coupled plasma atomic emission spectrometry (Optima 3000, Perkin Elmer).

The initial concentration of $H_2O_2$ was determined according to the method described by Olasehinde *et al.* (2008) based on the reduction of $H_2O_2$ by ferrous iron ($Fe^{2+}$) in acid solution to yield $^\bullet OH$ which is scavenged by benzene to produce phenol and analyzed by isocratic HPLC (LC-10Ai, Shimadzu) with fluorescence detector (Ex= 270nm and Em=298 nm) (reactions 9 and 10).

$$Fe^{2+} + H_2O_2 \rightarrow Fe^{3+} + {}^\bullet OH + OH^- \tag{9}$$

$${}^\bullet OH + C_6H_6 \rightarrow C_6H_5OH \tag{10}$$

The amount of phenol produced is directly proportional to the original amount of $H_2O_2$ present in the sample.

## 2-2-6- Photochemical Experiments: OH radical measurement

$^\bullet OH$ formation rate ($R_{OH}$) from the photo-Fenton reaction and total $R_{OH}$ were determined by HPLC-fluorescence detection (RF-10A, Shimadzu) following irradiation of the extracted sample using a solar simulator (Model 81160-100, Oriel Corp.) unit equipped with a 300 W Xenon lamp (ozone free, model 6258, Oriel Corp.). During photolysis, sample solutions were stirred by a magnetic stirrer covered with Teflon and maintained at a constant temperature of 20 °C using a circulator (RTE-111, NESLAB) and a chemical trap of photoformed $^\bullet OH$ with benzene probe (1.2 mM) according to the methodology described by Faust and Allen (1993) (Fig.2-4). This simple methodology has been used for the determination of $^\bullet OH$ formation rate in rain, dew and cloud water (Arakaki and Faust, 1998; Arakaki *et al.*, 1998).

Benzene is a suitable compound for this investigation because it undergoes fast reaction with OH (rate constant 7.8 x $10^9$ $M^{-1}$ $s^{-1}$, Buxton *et al.*, 1988) does not absorb lamp radiation and does not alter either the pH or the buffer capacity of the solutions.

Therefore, $R_{OH}$ was then determined using the following equation 11:

$$R_{OH} = (R_p/F_{b\text{-}OH} \ Y_p) \qquad (11)$$

where $R_p$ is the photochemical formation rate of phenol obtained experimentally, $F_{b\text{-}OH}$ is the fraction of •OH that react with benzene, as opposed to with other competing •OH scavengers, and $Y_p$ is the chemical yield of phenol from the reaction of •OH with the added benzene. $Y_p$ was reported to be 0.75. $F_{b\text{-}OH}$ for cloud water, reported by Arakaki and Faust (1998), was at least 0.94 with 1.2 mM added benzene, suggesting that most of the •OH formed photochemically in cloud water reacted with benzene.

The initial concentration of the added benzene in the WSF solution was 20 mM. Phenol was measured using isocratic HPLC with a pump (LC 10 Ai; Shimadzu), a C-18 column (LC-18 5 μm 4.6 mm i.d. x 250mm, Supelco or RP-18 GP 5μm 4.6 mm i.d. x 150 mm length, Kanto Kagaku) was used for separation and a fluorescence detector ($\lambda_{Ex}$270/$\lambda_{Em}$ 298 nm; RF-10A, Shimadzu). The mobile phase was acetonitrile and Milli-Q water [CH$_3$CN:H$_2$O 60:40] (v/v) and the flow rate 1.0 mL min$^{-1}$.

The concentrations of phenol were determined based on calibration curves made with Milli-Q water on the day of the illumination experiments. The initial formation rate of phenol ($R_p$, M min$^{-1}$) during an illumination experiment was determined from the plot of phenol concentrations versus illumination time using a linear regression analysis.

The light intensity of the solar simulator was controlled measuring the photochemical degradation rate of 2-nitrobenzaldehyde (2-NB) (chemical actinometer) by isocratic HPLC with UV detection of the absorbance wavelength set at 260 nm. The mobile phase and the flow rate were the same as for the determination of •OH. The degradation rate of 8μm 2-NB ($J_{2\text{-}NB}$) solution was normalized against a degradation rate of $J_{2\text{-}NB}$ = 0.00923 s$^{-1}$, which

was determined at noon under clear sky conditions in Higashi-Hiroshima city (34ºN) on 1 May of 1998 (Arakaki *et al*., 1998).

The contribution of the photo-Fenton reaction was determined based on the difference between the $^\bullet$OH formation rates with and without the addition of deferoxamine mesylate (DFOM) (Sigma Aldrich, Japan). The addition of DFOM produces a stable and strong complex with Fe (III) that results in suppression of the photo-Fenton reaction (Nakatani *et al.* 2007). Next, 1 µM potassium trioxalate ferrate (III) is added to the solution of the WSG fraction with 0.5 µM $H_2O_2$ with and without 10 µM DFOM to determine the potential for generation of $^\bullet$OH from the photo-Fenton reaction (reactions 12 to 14).

$$\text{Fe (III)-(DOM)}_m + \text{light} \rightarrow \text{Fe (II)-DOM}_{m-1} + \text{DOM}_{ox}^+ \quad\quad (12)$$

$$\text{Fe (OH)}^{2+} + \text{light} \rightarrow \text{Fe (II)} + {}^\bullet\text{OH} \quad\quad (13)$$

$$\text{Fe (II)} + H_2O_2 \rightarrow \text{Fe (III)} + {}^\bullet\text{OH} + \text{OH}^- \quad\quad (14)$$

The initial concentration of $H_2O_2$ was determined according to the method described by Olasehinde *et al.* (2008) based on the reduction of $H_2O_2$ by ferrous iron in acid solution to yield $^\bullet$OH which is scavenged by benzene to produce phenol and analyzed by HPLC with fluorescence detector (reactions 15 and 16).

$$Fe^{2+} + H_2O_2 \rightarrow Fe^{3+} + {}^\bullet\text{OH} + \text{OH}^- \quad\quad (15)$$

$${}^\bullet\text{OH} + C_6H_6 \rightarrow C_6H_5OH \quad\quad (16)$$

The amount of phenol produced is directly proportional to the original amount of $H_2O_2$ present in the sample. The total dissolved iron was determined using inductively coupled plasma atomic emission spectrometry (Optima 7300-DV, Perkin Elmer).

**2-2-7- Contribution of major sources of •OH (%)**

The contributions of various sources to •OH photoproduction were estimated. The percent contributions ($fi$) from well-known •OH sources, such as $NO_3^-$, $NO_2^-$ and $H_2O_2$ to total •OH formation ($fi$ ($I=NO_3^-$, $NO_2^-$ and $H_2O_2$)) can be calculated by the following equation 17:

$$fi = \frac{ki[Ci]}{R\text{total}} x100(\%) \qquad (i=NO_3^-, NO_2^- \text{ and } H_2O_2) \qquad (17)$$

where $ki$ is the rate of •OH formation from nitrate ($k_{NO3-} = 2.43 \times 10^{-7}$ s$^{-1}$), nitrite ($k_{NO2-} = 2.81 \times 10^{-5}$ s$^{-1}$) and hydrogen peroxide ($k_{H2O2} = 3.52 \times 10^{-6}$ s$^{-1}$), [$C_i$] is the concentration of each species and $R_{OHtotal}$ is the •OH photoproduction rate determined experimentally for the sample (Arakaki *et al.*, 1998; Nakatani *et al.*, 2001).

**2-2-8- Fluorescence Properties**

To estimate the unknown sources of •OH, the fluorescence matter (FM) was investigated based on the 3D-excitation emission matrix (EEM) spectrum obtained using a fluorescence spectrometer (F-4500, Hitachi, Ltd.). The samples were scanned at excitation wavelengths of 225-400 nm and emission wavelengths of 250-500 nm at intervals of 5 nm and a scanning speed of 1200 nm.min$^{-1}$ to obtain the overall characteristics. The samples were calibrated using 2.8 μg L$^{-1}$ of quinine sulfate dehydrated solution (Nacalai Tesque) as a standard for fluorescence intensity (FI), which corresponds to 25 fluorescence units (flu).

**2-2-9- Air mass backward trajectory analysis**

Air mass backward trajectories were analyzed using the North American simulator HYSPLIT model (Hybrid Single-Particle Lagrangian Integrated Trajectory) from the Air Resources Laboratory (ARL) of National Oceanic and Atmospheric

Administration (NOAA, 2010), available online. Using a mathematical dispersion model, simple to complex windy trajectories can be simulated (Draxler, 1998). Setting up the parameters such as trajectory direction (backward), start time (day and time), total run time (total sampling duration) and new trajectory frequency (represents the color trajectories traced every 6 hours totalizing 24 trajectories), the wind backward can be traced and investigated. The occurrence of the Yellow Sand event was monitored by the Japan Meteorology Agency (2010).

## 2-3- Results and Discussion

### 2-3-1- Chemical composition of WSG and WEA fractions

Among the major anions present in the WSG and WEA samples, $SO_4^{2-}$ was the most abundant. The mean concentration of $SO_4^{2-}$ was 9.4±4.0 nmol m$^{-3}$ in the WSG and 81±33 nmol.m$^{-3}$ for the WEA. This was followed by $NO_3^-$, which was present at mean concentrations of 9.3±4.1 nmol m$^{-3}$ for the WSG and 47±32 nmol m$^{-3}$ for the WEA fraction. The $NH_4^+$ concentration was the highest among the measured cations, being present at a mean concentration of 8.4±9.4 nmol m$^{-3}$ in the WSG and 84±42 nmol m$^{-3}$ in the WEA samples. The total concentrations of anions found in the WEA fraction were about five times higher than those found in the WSG fraction. The WSG fraction showed that metal species such as $Na^+$, $K^+$, $Ca^{2+}$, and $Mg^{2+}$ were contaminated from the impinger and other instruments in the collection device, resulting in apparent presence of those metals in the WSG fraction. Therefore the data of metal species in the WSG fraction was omitted from our results. Iron and other heavy metals were not detected in the WSG fraction. The mean initial concentration of $H_2O_2$ was 0.2±0.3 nmol m$^{-3}$ in the WSG and 0.9±2.3 nmol m$^{-3}$ in the WEA fraction. DOC, which was determined for WSG fraction only, due to the scarce

volume of WEA sample, ranged from 0.1 to 5.3 mg C m$^{-3}$ with a mean of 2.9±2.6 mg C m$^{-3}$ (Table 2-1).

## 2-3-2- $^\bullet$OH photoformation rate (R$_{OH}$)

$^\bullet$OH was detected in all 24 samples and was found to increase linearly with increasing illumination time in both fractions (WEA and WSG) (Figure 2-5). These findings show the same photochemistry occurring in both fractions on $^\bullet$OH generation in the aqueous phase.

The $^\bullet$OH photoformation rate was found to range from 0.04 to 2.5 nmol h$^{-1}$ m$^{-3}$ with a mean of 0.5 nmol h$^{-1}$ m$^{-3}$ for the WSG fraction and from 0.1 to 8.4 nmol h$^{-1}$ m$^{-3}$ with a mean of 1.4 nmol.h$^{-1}$m$^{-3}$ for the WEA sample. The $^\bullet$OH photoformation rates in the WSG fractions collected during this study are summarized in Table 2-2 and compared with those of other studies. Analyses in the other studies were conducted using the same conditions to irradiate samples (simulated sunlight), except for the Okinawa and Canada studies, in which a monochromatic light adjusted to 313 nm was used.

The $^\bullet$OH photoformation rate determined in this study revealed that the WEA photoformation rate was about three times higher than that of the WSG fraction, and was much higher (more than one magnitude) than previously reported R$_{OH}$ values for the WEA fraction. The $^\bullet$OH formation rate of the WSG fraction was even higher than that of the R$_{OH}$ in the WEA fraction obtained by other investigators.

Once the mean R$_{OH}$ in the WEA is shown higher than the WSG fraction in this study, there is a hypothesis that the WEA fraction contains larger source compounds of $^\bullet$OH than the WSG fraction.

### 2-3-3- Contribution of major sources of $^{\bullet}OH$

In the WSG fraction, the presence of $NO_3^-$, $NO_2^-$ and $H_2O_2$ detected in most of the samples contributed only a relatively low percentage of the $^{\bullet}OH$ photoformation when compared to the unknown sources (Table 2-3). The contributions of the major sources of $^{\bullet}OH$ generation in the WSG fraction were found to be 4.5% for $NO_3^-$, 0.7% for $NO_2^-$ and 1.2% for $H_2O_2$. Majority of $^{\bullet}OH$ sources is, therefore, unknown. In this study, an experiment was carried out to elucidate the sources of $^{\bullet}OH$. Photo-Fenton reaction was examined because this reaction is considered to be a major $^{\bullet}OH$ source in both atmospheric aqueous phase and natural water (Nakatani *et al*. 2007). Dissolved iron species are common to exist in atmospheric aqueous phase (Kim *et al*. 2001, 2003). If water soluble gases meet with iron species in the aqueous phase photo-Fenton reaction may occur. To find potential sources of $^{\bullet}OH$ in the atmospheric aqueous phase, known amount (excess) of iron (III) was added into the solution of the WSG fraction and then the $R_{OH}$ of photo-Fenton reaction was determined by the method of Nakatani *et al.* (2007). The results indicated that the photo-Fenton reaction contributed up to 42% of the total $^{\bullet}OH$ photoformation in the WSG fraction while remaining unknown sources accounted for 52% of the photo-formations (Table 2-3). In a previous study conducted by Kondo *et al.* (2009), the photo-Fenton reaction was found to contribute 49% of the $^{\bullet}OH$ photoformation in the WEA fraction collected at Higashi-Hiroshima during 2003-2007 (n=23). Therefore the photo-Fenton reaction may be a significant contributor of $^{\bullet}OH$ in the aqueous phase of ambient air, as well as river and rainwaters, as summarized in Table 2-3.

In the WEA fraction, $NO_3^-$, $NO_2^-$, $H_2O_2$ and unknown sources accounted for 8.9, 1.2, 2.5 and 87% of the $^{\bullet}OH$ photoformed, respectively (Table 2-3). However, photo-Fenton reaction was not analyzed in the WEA fraction due to lack of sufficient amount of air

samples for the analysis and thus the unknown sources are supposed to contain photo-Fenton reaction.

**2-3-4- HULIS as unknown sources of $^{\bullet}$OH**

Fluorescence properties were higher present in the WEA than the WSG fractions. Among the 24 samples collected, 24 WEA samples showed fluorescent properties while in the WSG, 22 samples (91%). For most of these samples, two peaks of fluorescence were detected. A fluorescence peak was observed at $\lambda_{Ex/Em}$=240–250/395–415nm (peak A), while a second peak was observed at $\lambda_{Ex/Em}$= 295–315/395–410 nm (peak B). Previous studies (Coble *et al.*, 1990; Coble, 1996; Parlanti *et al.*, 2000; Zepp *et al.*, 2004; Graber and Rudich, 2006) found that HULIS had two distinctive peaks, whose Ex/Em wavelengths are similar to those of the two peaks found in this study, suggesting the presence of HULIS in both WEA and WSG fractions (Figure 2-6).

The mean fluorescence intensities of the peak A were 54±122 flu for the WSG and 316±116 flu for the WEA while those of the peak B were72±170 flu for the WSG and 311±136 flu for the WEA fractions. Larger abundance of the two peaks in the WEA fraction than the WSG fraction was associated with higher photoformation rate of $^{\bullet}$OH in the former fraction than the latter fraction, suggesting that HULIS may be the "unknown sources" of $^{\bullet}$OH. Kondo *et al.* (2009) suggested that WEA samples collected at same sampling site as this study contains unidentified compounds which could be fluorescent organic compounds, such as HULIS. They found liner correlations of the fluorescence intensities of the peak A and B with the photoformation rate of $^{\bullet}$OH from the unknown sources. Possible presence of HULIS in the WSG fractions leads to the discussion that some HULIS perhaps exist as a low molecular size and existed in the WSG fraction.

Presently no conclusive data of HULIS, other than the 3D-EEM spectra, are available and thus further study needs to confirm it.

**2-3-5- Monthly variations in the $R_{OH}$ and other chemical compounds**

Figure 2-7a shows the $^\bullet$OH photoformation rate and the concentrations of $SO_4^{2-}$, $NH_4^+$, $NO_3^-$ and DOC per month in the WSG fraction. The $R_{OH}$ determined for the samples collected in June, July and September of 2008 revealed increasing rates of $^\bullet$OH generation and after that shown to be a decreasing trend. The sample collected in the September, 2008 showed the highest, $R_{OH}$ =2.5 nmol h$^{-1}$ min$^{-1}$. Low contributions from $NO_2^-$ (0.17%), $NO_3^-$ (0.55%) and $H_2O_2$ (0.01%) and high contribution from unknown sources (50.3%) in September 2008 explained the highest $R_{OH}$ among the 24 samples. During 2009-2010 $^\bullet$OH photoformation rate was low (<0.5nmol m$^{-3}$) and flat. There were no clear relations between $R_{OH}$ and concentrations of other analytical items.

The $R_{OH}$ variations in the WEA fractions were observed higher in the samples collected in 11-18 March, 23-30 April and 20-27 May of 2010 (Figure 2-7b). The Yellow Sand (Asian Aeolian Dust) events were occurred in the sampling date of 11-21 February and 16-18 March of 2009, and 13-16 March, 27-30 April and 21-25 May of 2010 (Japan Meteorological Agency, 2010). Air masses from continental China brought large amounts of yellow Sand and the concentrations of $SO_4^{2-}$ and $NH_4^+$ appeared to be relatively high during the event. As Arakaki *et al.* (2006) reported that a few WEA samples collected in Okinawa were affected by a Yellow Sand event, which resulted in increased $^\bullet$OH photoformation, there is a hypothesis about the possible influence of long-range transport of air masses (from the Asia continent) increasing the $^\bullet$OH formation rate. In this study, even though a similar phenomenon was observed as the Arakaki *et al.* reported, the $R_{OH}$ was not always following the monthly variations of $SO_4^{2-}$ and $NH_4^+$, which suggests that

other factors may also be involved in the photoformation of $^\bullet$OH in the WEA fraction. Lack of a number of Yellow Sand event observed (5 events) at Higashi-Hiroshima and/or possible mixing of domestic pollutants in Japan with long-range transported ones may cause a difficulty in evaluating effects of Yellow Sand event to the $R_{OH}$ (Figure 2-8).

**2-4- Conclusions**

The $^\bullet$OH photoformation rate, its generation sources and source strength for the WEA and WSG fractions in ambient air of Higashi-Hiroshima were studied from June 2008 to June 2010. To the best of our knowledge, this study reports the first findings regarding $^\bullet$OH generation in WSG fractions collected from ambient air. $^\bullet$OH photoformation rate in WSG fractions may be useful as an indicative of amount of $^\bullet$OH generation sources and oxidation capacities of ambient air. A linear relationship between the $^\bullet$OH generation and irradiation time in the photochemical experiments showed that both fractions have the same photochemistry of $^\bullet$OH generation. The results also revealed that among the major sources of $^\bullet$OH, the photo-Fenton reaction and unknown sources were the most important sources of $^\bullet$OH. The unknown source may be fluorescent organic matter such as HULIS. However, a further research focusing on organic matter and the relationship with $^\bullet$OH generation in the WSG fraction is need and expected to continue.

# References

Anastasio, C., Faust, B. C. and Allen, J. M., 1994. Aqueous-phase photochemical formation of hydrogen-peroxide in authentic cloud waters, Journal of Geophysical Research-Atmospheres, 99, 8231–8248.

Anastasio, C. and Jordan, A.L., 2004. Photoformation of hydroxyl radical and hydrogen peroxide in aerosol particle from Alert, Nunavut: implications for aerosol and snowpack chemistry in the Artic. Atmospheric Environment 38, 1153-1166.

Anastasio, C. and Newberg, J.T., 2007. Sources and sinks of hydroxyl radical in sea-salt particles. Journal of Geophysical Research 112, D10306, doi:10.1029/2006JD008061.

Arakaki, T. and Faust, B.C., 1998. Sources, sinks, and mechanisms of hydroxyl radical (OH) photoproduction and consumption in authentic acidic continental cloud waters from Whiteface in Mountain, New York: the role of the Fe(r) (r = II, III) photochemical cycle. Journal of Geophysical Research 103 (D3), 3487-3504.

Arakaki, T., Miyake, T., Shibata, M. and Sakugawa, H., 1998. Measurement of photochemically formed hydroxyl radical in rain and dew waters. The Chemical Society of Japan, 9, 619-625 (in Japanese).

Arakaki, T., Kuroki, Y., Okada, K., Nakama, Y., Ikota, H., Higuchi, T., Uehara, M., Tanahara, A., 2006. Chemical composition of photochemical formation of hydroxyl radical in aqueous extracts of aerosol particles collected in Okinawa, Japan. Atmospheric Environment 40, 4764-4774.

Buxton, G.V., Greenstock, C.L., Helman, W.P., Ross, A.B., 1988. Critical review of rate constants for reactions of hydrated electrons, hydrogen atoms and hydroxyl radicals ($^\bullet$OH /$^\bullet$O$^-$) in aqueous solution. J. Phys. Chem. Ref. Data17, 513-886.

Coble, P.G.; Green, S.A.; Blough, N.V.; Gagosian, R.B., 1990. Characterization of dissolved organic matter in the Black Sea by fluorescence spectroscopy. Nature 348 (6300), 432-435.

Coble, P.G., 1996. Characterization of marine and terrestrial DOM in sea water using excitation-emission matrix spectroscopy. Marine Chemistry 51, 325-346.

Draxler, R.R., 1998. An overview of the HYSPLIT_4 Modeling System for Trajectories, Dispersion, and Deposition. Australian Meteorological Magazine, 45, 295-308.

Faust, B.C. and Allen, J.M., 1993. Aqueous-phase photochemical formation of hydroxyl radical in authentic cloudwaters and fogwaters. Environmental Science and Technology 27, 1221-1224.

Faust, B.C., Anastasio, C., Allen, J.M., Arakaki, T., 1993. Aqueous-phase photochemical formation of peroxides in authentic cloud and fog waters. Science 260, 73-75.

Finlayson-Pitts, B. J. and Pitts, James N. Jr., 1986. Tropospheric air pollution: ozone, airborne toxics, polycyclic aromatic hydrocarbons, and particles. Atmospheric Chemistry, Wiley-Interscience, New York, 667-724.

Graber, E. R. and Rudich, Y., 2006. Atmospheric HULIS: How humic-like are they? A comprehensive and critical review. Atmospheric Chemistry and Physics 6, 729-753.

Japan Meteorological Agency, 2010. Aeolian Dust Information. http://www.data.kishou.go.jp/obs-env/kosahp/kosa_table_1.html (in Japanese)

Kim, D.H., Takeda, K., Sakugawa, H., Lee, J.S., 2001. The determination of dissolved total Fe by flow injection analysis in environmental samples. Analytical Science & Technology Vol. 14 (6), 510-515.

Kim, D.H., Takeda, K., Sakugawa, H., Lee, J.S., 2003. The photochemical reactions of iron species in rain and snow in Higashi-Hiroshima, Japan. Analytical Science & Technology Vol. 16 (6), 466-474.

Kondo, H., Chiwa, M., Sakugawa, H., 2009. Photochemical formation and scavenging mechanisms of hydroxyl radical in water-extracts of atmospheric aerosol collected in Higashi-Hiroshima, Japan. Geochemistry 43, 15-25 (in Japanese).

Nakatani, N., Miyake T., Chiwa, M., Hashimoto, N., Arakaki, T. and Sakugawa, H., 2001. Photochemical formation of OH radicals in dew formed on the pine needles at Mt. Gokurakuji. Water, Air and Soil Pollution 130: 397-402.

Nakatani, N., Ueda, M., Shindo, H., Takeda, K. and Sakugawa, H., 2007. Contribution of the Photo-Fenton reaction to hydroxyl radical formation rates in river and rain water samples. Analytical Sciences, 23, 1137-1142.

National Oceanic and Atmospheric Administration (NOAA), HYSPLIT trajectory model simulator. http://ready.arl.noaa.gov/HYSPLIT.php

Olasehinde, E.F., Makino, S., Kondo, H., Takeda, K., Sakugawa, H., 2008. Application of Fenton reaction for nanomolar determination of hydrogen peroxide in seawater. Analytica Chimica Acta, 627, 270-276.

Parlanti, E., Wörz, K., Geoffroy, L., Lamotte, M., 2000. Dissolved organic matter fluorescence spectroscopy as a toll to estimate biological activity in a coastal zone submitted to anthropogenic inputs. Organic Geochemistry 31 (12), 1765-1781.

Zepp, R.G., Sheldon, W.M., Moran, M.A., 2004. Dissolved organic fluorophores in southeastern US coastal waters: correction method for eliminating Rayleigh and Raman scattering peaks in excitation-emission matrices. Marine Chemistry 89 (1-4), 15-36.

**Table 2-1.** Chemical composition and mean concentration of WEA and WSG fractions extracted from air samples collected during 2008 - 2010 in Higashi-Hiroshima, Japan

| | WEA (mean± SD) | Range | WSG (mean± SD) | Range |
|---|---|---|---|---|
| $Cl^-$ (nmol m$^{-3}$) | 25±18 | 4.2 – 66 | 9.4±4.0 | 0.3 - 16 |
| $NO_3^-$ (nmol m$^{-3}$) | 47±32 | 13 – 148 | 9.3±4.1 | 2.1 – 19.7 |
| $NO_2^{-*}$ (nmol m$^{-3}$) | 0.07±0.06 | ND-0.14 | 0.03±0.016 | ND-0.04 |
| $SO_4^{2-}$ (nmol m$^{-3}$) | 81±33 | 20 – 150 | 9.4±4.0 | 0.2 – 16.6 |
| $NH_4^+$ (nmol m$^{-3}$) | 84±42 | 31 –227 | 8.4±9.4 | ND – 35 |
| $Na^+$ (nmol m$^{-3}$) | 56±30 | 24 –151 | NA | NA |
| $K^+$ (nmol m$^{-3}$) | 29±19 | 7.5– 78 | NA | NA |
| $Ca^{2+}$ (nmol m$^{-3}$) | NA | NA | NA | NA |
| $Mg^{2+}$ (nmol m$^{-3}$) | 7.6±4.1 | 2.8– 17 | NA | NA |
| DOC (mg C m$^{-3}$) | NA | NA | 2.9±2.6 | 0.1 – 5.3 |
| $H_2O_2$ (nmol m$^{-3}$) | 0.9±2.3 | 0.01 - 11 | 0.2±0.3 | 0.02– 1.0 |

*Note:* NA: not analyzed     ND: not detected     SD: standard deviation

**Table 2-2.** OH radical photo formation rate in WEA and WSG fractions

| Site | Light [b] | n | $R_{OH,air}$ (nmol h$^{-1}$ m$^{-3}$) | | | | References |
| | | | Mean WEA | Range WEA | Mean WSG | Range WSG | |
|---|---|---|---|---|---|---|---|
| Higashi-Hiroshima, Japan | Solar | 24 | 1.4[a] | 0.1-8.4 | 0.5 | 0.04-2.5 | *This Study* |
| Higashi-Hiroshima, Japan | Solar | 41 | 0.33[a] | 0.02-1.91 | -[c] | -[c] | Kondo *et al.*, 2009 |
| Bodega Bay, California, USA | Solar | 1 | 0.092 | - | -[c] | -[c] | Anastasio and Newberg,2007 |
| Alert, Canada | 313 | 2 | 0.010 | 0.008-0.013 | -[c] | -[c] | Anastasio and Jordan, 2004 |
| Okinawa, Japan | 313 | 14 | 0.11 | ND-0.21 | -[c] | -[c] | Arakaki *et al.*, 2006 |

*Note: [a] Normalized to $J_{2-NB}$ = 0.0093 s$^{-1}$ [b] Light used to irradiate sample (simulated light) [c] no data*

**Table 2-3.** The contribution of major sources of OH radical to the atmospheric WEA and WSG fractions, as well as river and rainwater collected in Higashi-Hiroshima, Japan (n=22)

| Site | n | $f_{NO3^-}$ | $f_{NO2^-}$ | $f_{H2O2}$ | $f_{Photo-Fenton}$ | $f_{Unknown}$ | References |
|---|---|---|---|---|---|---|---|
| | | | | Contribution, %[a] | | | |
| Higashi-Hiroshima, Japan (WSG) | 24 | 4.5 | 0.7 | 1.2 | (42)[b] | 52 | *This study* |
| Higashi-Hiroshima, Japan (WEA) | 24 | 8.9 | 1.2 | 2.5 | | (87)[c] | *This study* |
| Higashi-Hiroshima, Japan (WEA) | 41 | 12 | 10 | 0.4 | 49[d] | 33[d] | Kondo *et al.*, 2009 |
| Higashi-Hiroshima, Japan (River) | 33 | 33 | 31 | <1 | 15 | 20 | Nakatani *et al.*, 2007 |
| Higashi-Hiroshima, Japan (Rain) | 9 | 10 | 16 | 37 | 21 | 16 | Nakatani *et al.*, 2007 |

Notes: [a]$f_i = [ki[Ci]/R_{OHtotal}] \times 100$ (%)    [b]Generation potential of $^{\bullet}$OH from photo-Fenton reaction
[c]$f_{Photo-Fenton} + f_{Unknown}$    [d]$n=23$
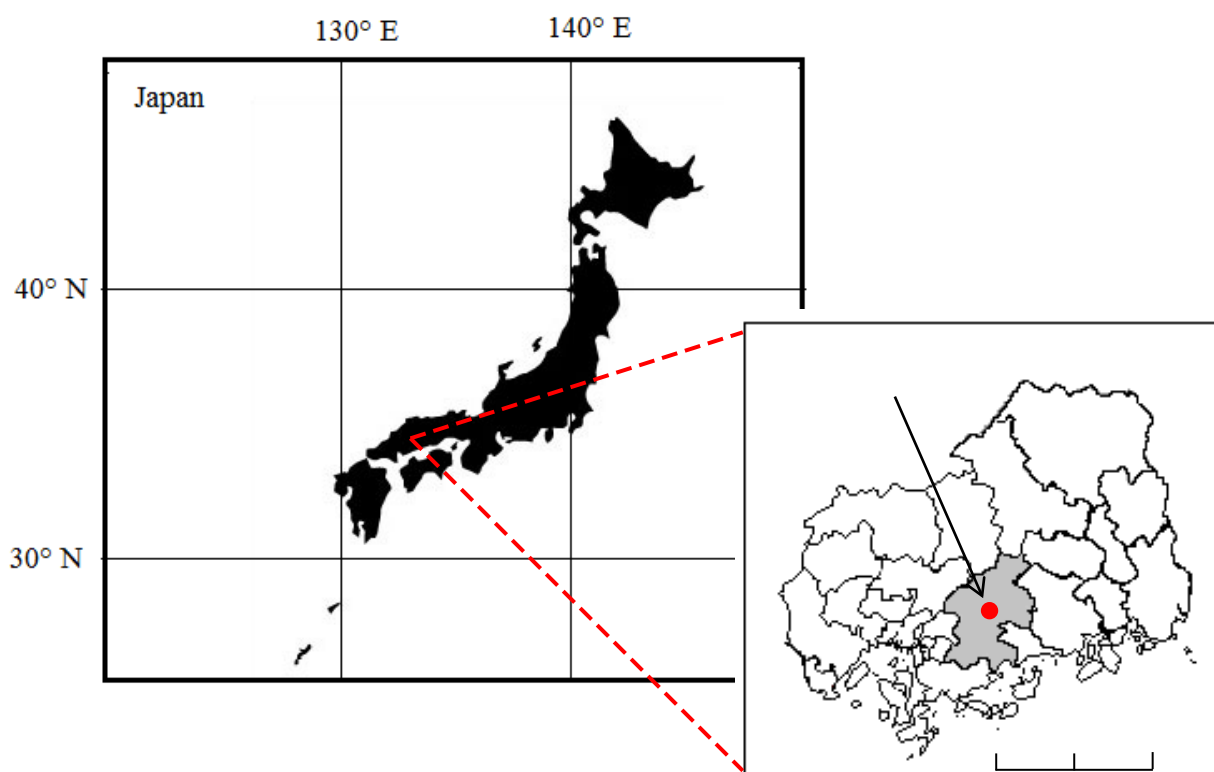
**Figure 2-1.** Sampling site of atmospheric aerosol particles and aqueous solution of water-soluble gas in Hiroshima prefecture
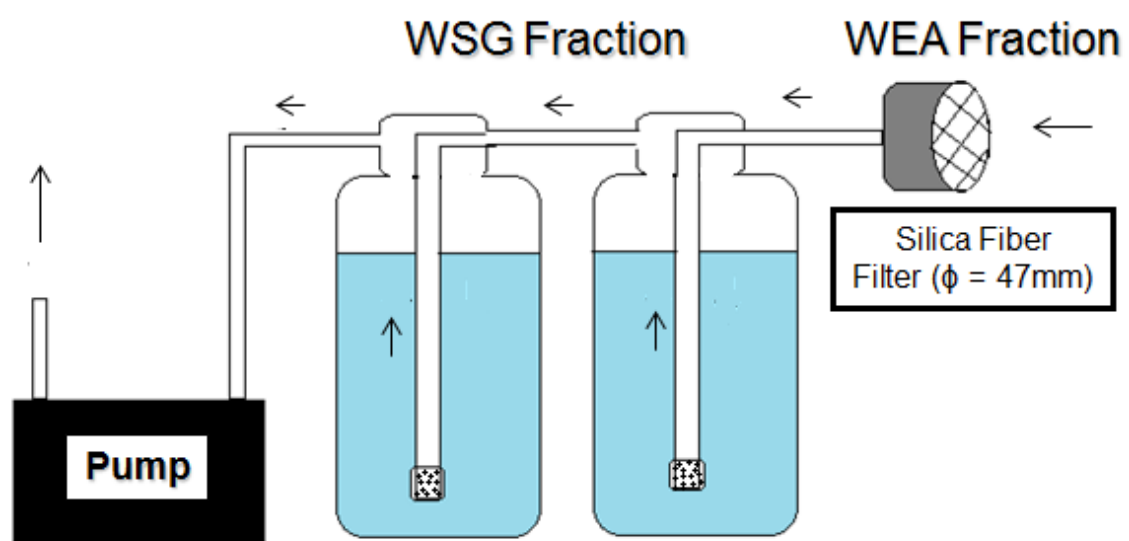
**Figure 2-2.** Sampling system of atmospheric aerosol particles and aqueous solution of water-soluble gas fractions (coupled low volume air sampler).
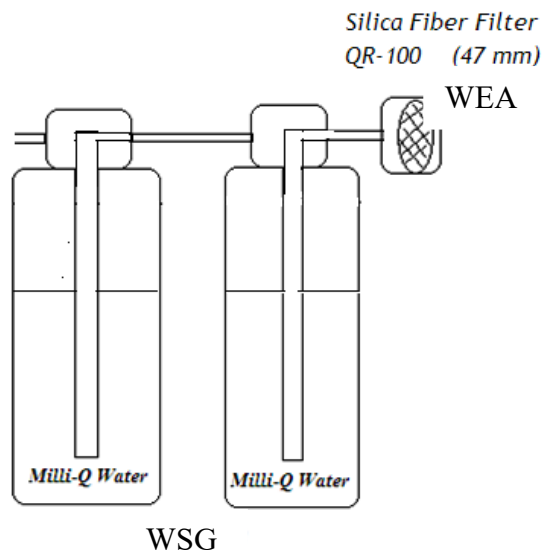
**Figure 2-3.** Blank control test (without pump connection)
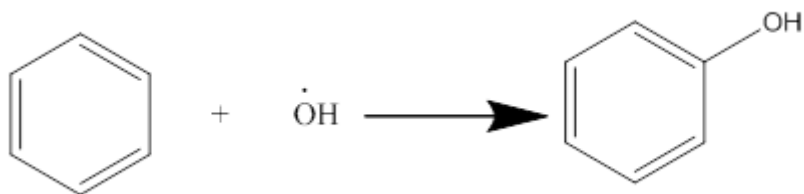


**Figure 2-4.** Benzene probe reaction to determine the $^\bullet$OH formation rate
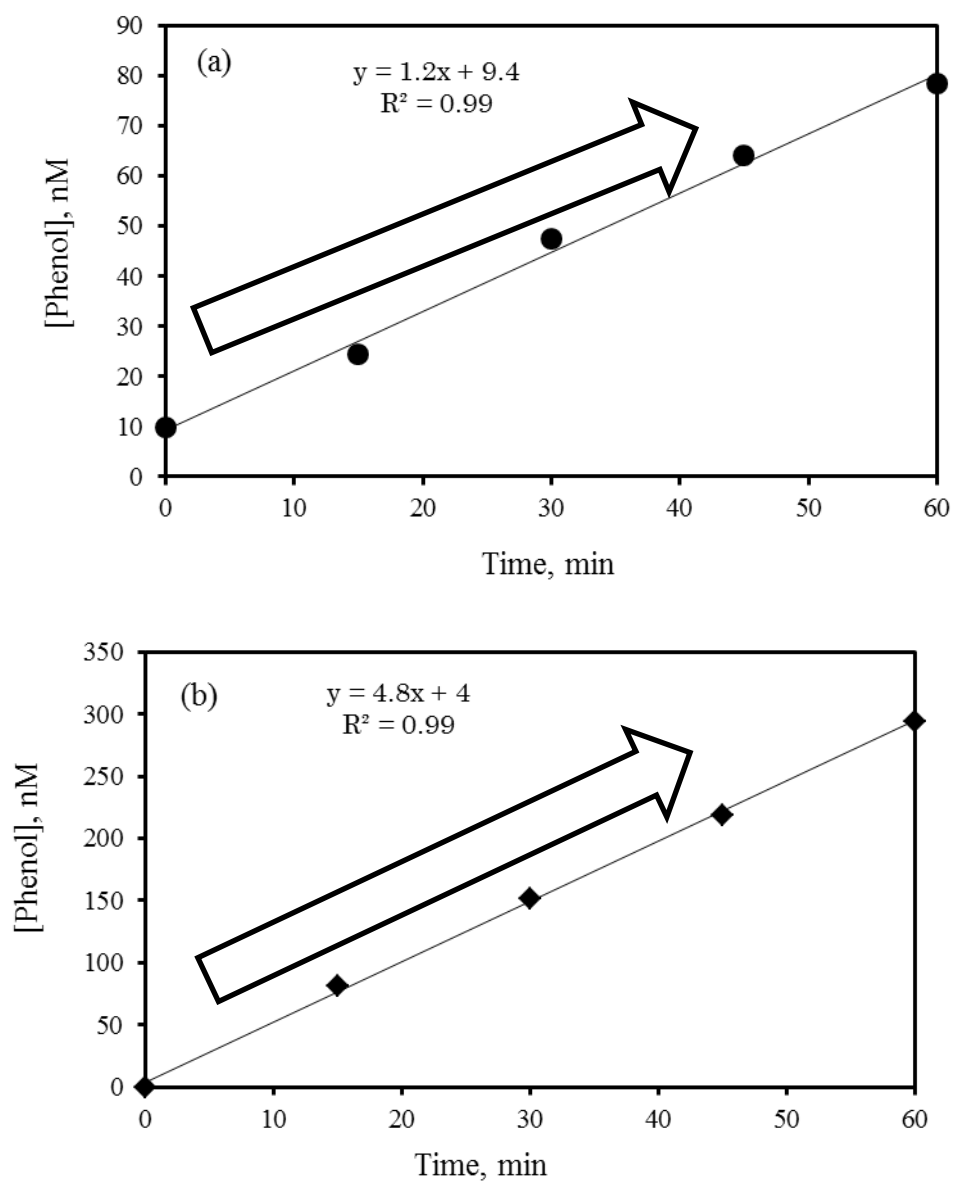
**Figure 2-5.** Photoformation rate of phenol in WSG (a) and WEA (b) fractions in the air

sample collected in August, 11 of 2009
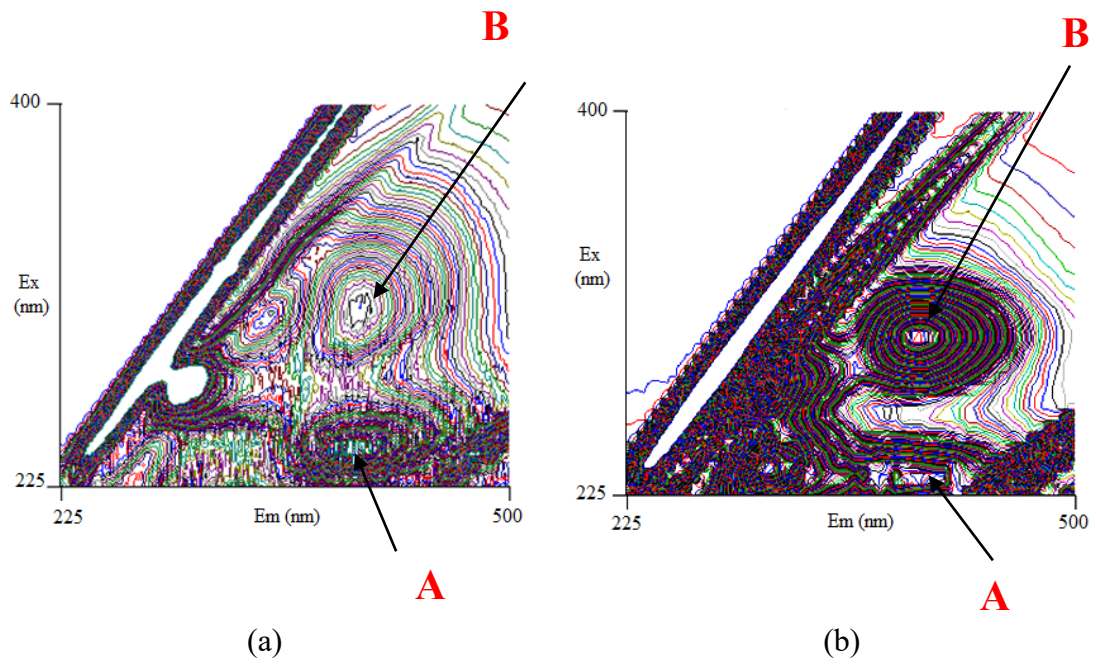
**Figure 2-6.** 3-D EEM spectrum of WEA sample collected in August 11, 2009 (a) and of WSG sample collected in June, 15, 2009 (b)
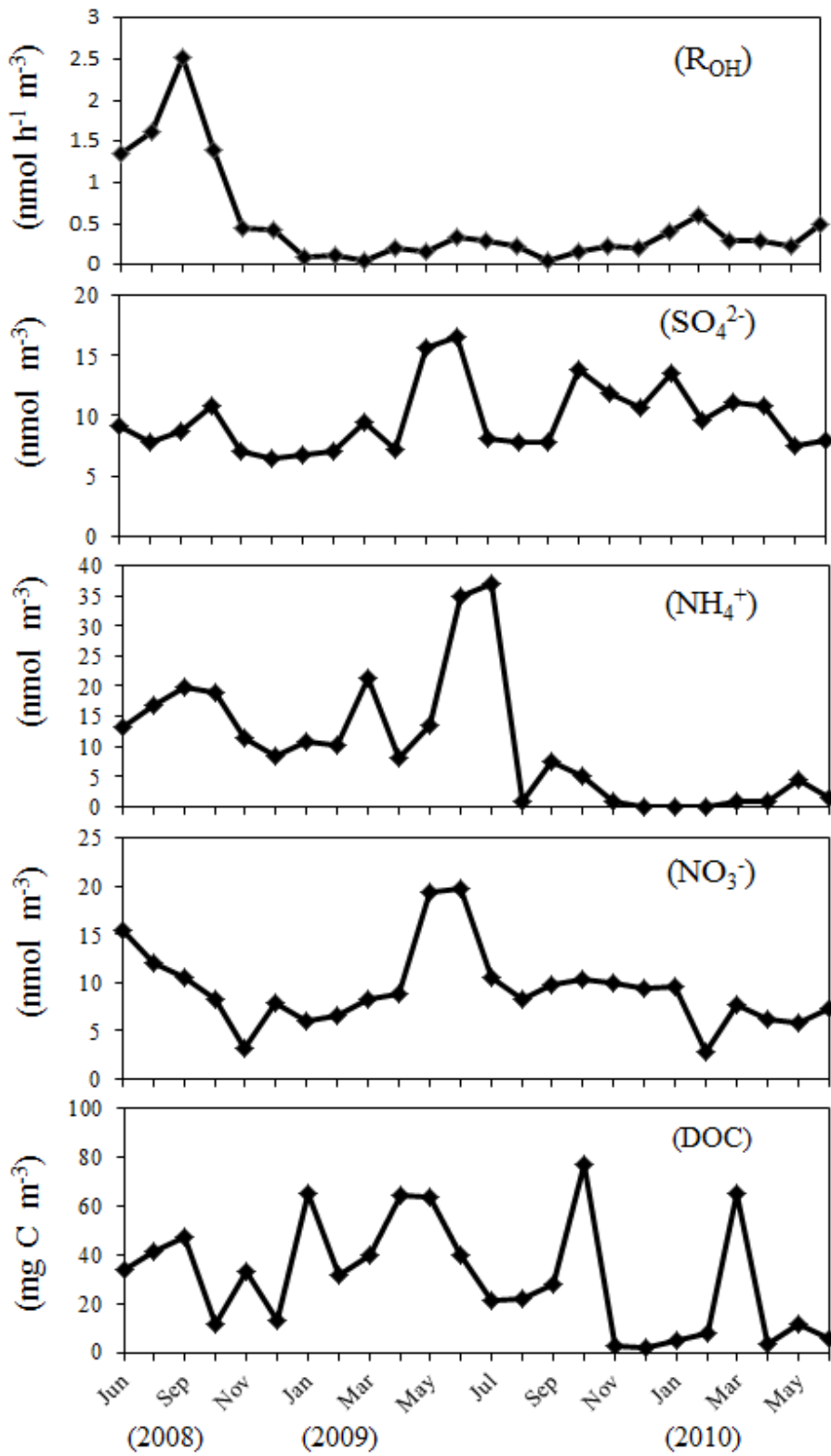
(a)
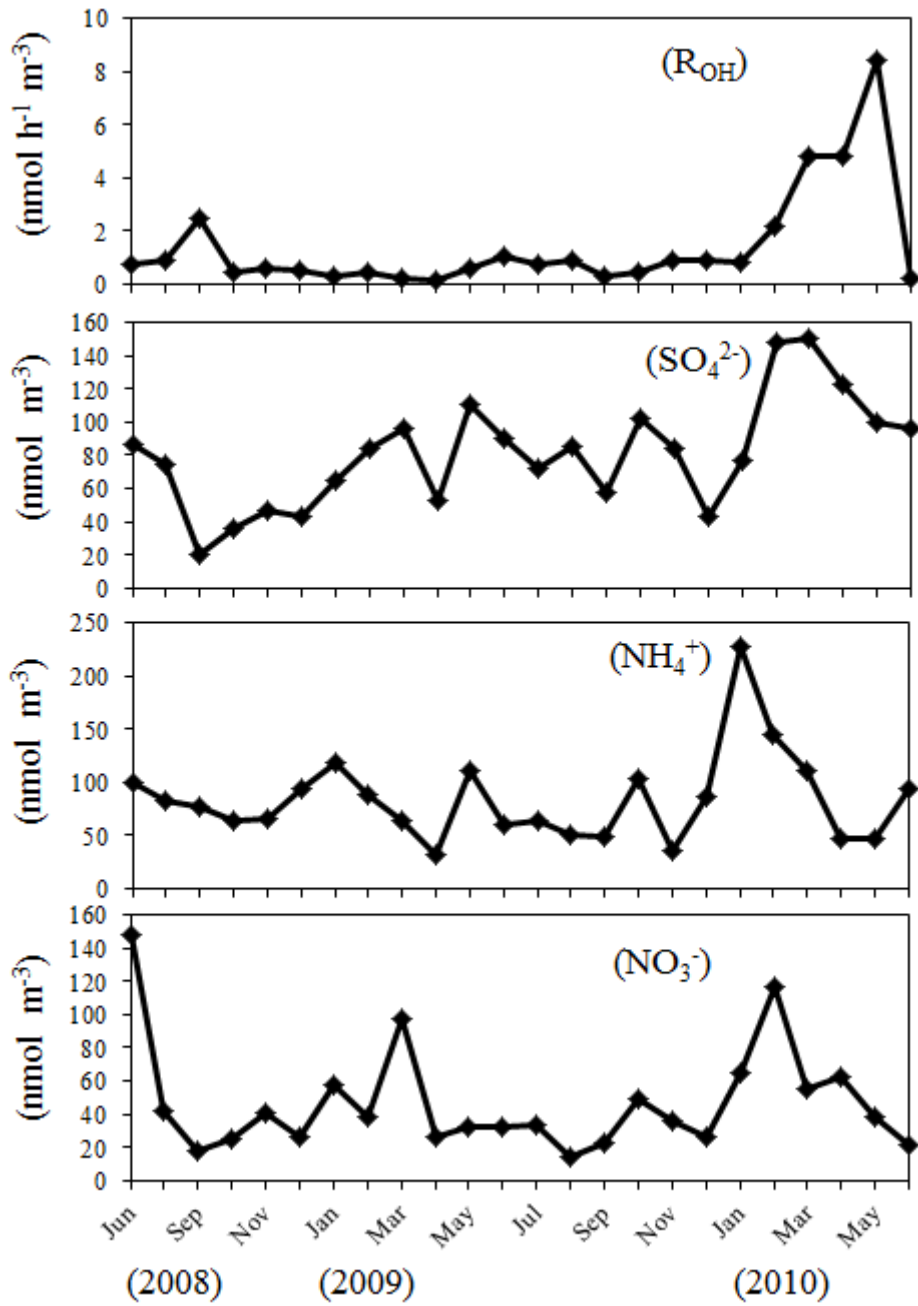
(b)

**Figure 2-7.** Variations in the photoformation rates of •OH and concentrations of inorganic ions and DOC in the WSG (a) and photoformation rates of •OH and concentrations of inorganic ions in WEA (b) samples collected during June 2008 - June 2010.
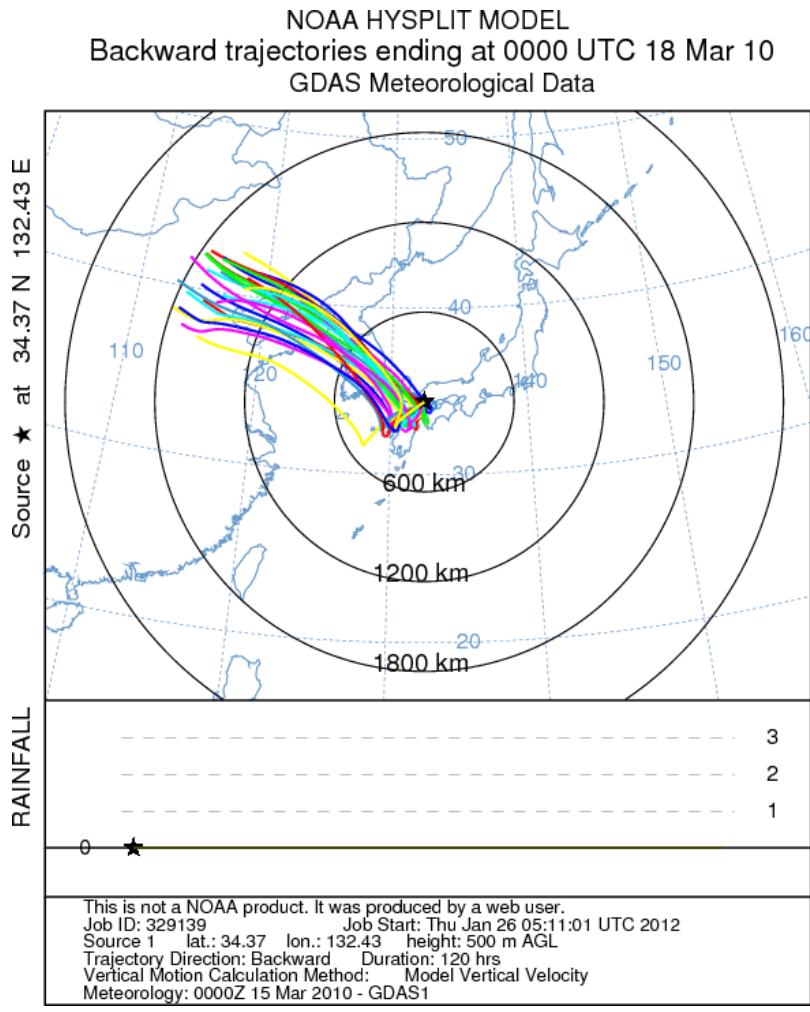
**Figure 2-8.** Wind back trajectory showing the possible influence of Yellow sand event affecting the oxidation capacity of $^\bullet$OH (March 18$^{th}$ /2010).

# Chapter 3

# Chapter 3

**Photochemical formation of OH radical in marine aerosols collected in Seto Inland Sea, Japan.**

## 3-1-Introduction

Aerosol particles consist of many natural and anthropogenic components, including mineral dust, soot, organic molecules, sea salt crystals, spores, bacteria, and other microscopic particles (Duce, 2005).

Given the ocean's extension, marine aerosol constitutes one of the most important natural aerosol systems at the global level (O'Dowd *et al.,* 2007). The literature contains a great deal of evidence that large sectors of the marine atmosphere are influenced by continental outflows (natural and anthropogenic) and by ship exhaust emissions (Chen *et al.,* 2005; Huang *et al.*, 2008).

According to Keene *et al.* (2007), the relative concentrations of inorganic constituents of nascent marine aerosols are similar to those in bulk seawater but organic matter (OM) is likely a major source of reactive species including the hydroxyl radicals ($^{\bullet}$OH) and hydroperoxides.

It's reported that $^{\bullet}$OH are photochemically generated in atmospheric hydrometeors (Faust *et al.*, 1993; Faust and Allen, 1993; Arakaki *et al.*, 1998; Arakaki and Faust, 1998; Anastasio *et al.*, 1994; Anastasio and McGregor, 2001; Arakaki *et al.*, 2006 and Kondo *et al.* 2009), as well as seawater, river water and lake water (Mopper and Zhou, 1990; Allen *et al.*, 1996; Vaughan and Blough, 1998; Qian *et al.*, 2001; White *et al.*, 2003; Takeda *et al.*, 2004; Vione *et al.*, 2006; Nakatani *et al.*, 2007). $^{\bullet}$OH can be generated in the aqueous phase through various photochemical reactions as we discussed in the *Chapter 2*, such as the photolysis of nitrate ($NO_3^-$), nitrite ($NO_2^-$ and $HNO_2$), hydrogen peroxide ($H_2O_2$), and aqueous iron complexes in the Fenton and photo-Fenton reaction (Mopper and Zhou, 1990).

To better assess the impact of marine aerosols on tropospheric chemistry and their overall oxidizing capacity in the troposphere, we need to understand the sources and fates of photoformed $^\bullet$OH in the aerosol. However, only few studies on the $^\bullet$OH photoformation rate in aqueous extract of marine aerosols had been conducted (Anastasio and Newberg, 2007) and no study regarding the $^\bullet$OH photogeneration in the samples collected in the Seto Inland Sea region has been done. Thus, this study focused on the determination of the $^\bullet$OH photoformation rate, chemical composition and the major sources of $^\bullet$OH in water-extracts of marine aerosol particles collected in the Seto Inland Sea region, in Japan.

## 3-2- Experimental

### 3-2-1- Sampling Area

Formally named the Seto Inland Sea (or Seto Naikai), the Inland Sea is the body of water separating Honshū, Shikoku, and Kyūshū, three of the main islands of Japan. It connects to Osaka Bay and provides a sea transport link to industrial centers in the Kansai region, including Osaka and Kobe (Figure 3-1). The Seto Inland Sea is well known to be one of the most industrially developed areas in Japan. Its length is about 500 km, its width 5 km to 50 km and its average depth about 30 m (Yanagi and Okaichi, 1997).

### 3-2-2- Sampling Methods

Marine aerosol particles were collected using a High Volume Sampler (HVS-500-5, Kimoto Electric Co. LTD, Japan) (Figure 3-2) in the research cruise of the Toyoshio Maru belonging to Hiroshima University during 13th -16th September 2010. Sixteen aerosol samples were collected during the cruise (n=16).

The sampler was set up on the front deck (5 m above sea level) of the ship and air filter used consisted of precombusted silica fiber filter (QR-100 203 x 254 mm, Advantec) operating at a constant flow rate of approximately 1 $m^3$ $min^{-1}$. All the samples, of which

average air volume was 113.3 m$^3$ (ranging from 30 to 240 m$^3$), were collected during daylight when the ship was running at regular speed (10 nautical mile or 5.38 m min$^{-1}$) in order to avoid smoke contamination from the ship's stack.

Each sample corresponds to certain trajectory on the cruise in the Seto Inland Sea, numbered according to Table 3-1 that describes the day, time, coordinates and corresponding area. Figure 3-3 illustrates the sampling trajectory during the research cruise.

The sampled filters were covered by aluminum foil and sealed in plastic bags and kept under refrigeration (≈4°C). A blank control filter was analyzed in the same manner as the aerosol filters. It was left on the non-operating sampler for a few minutes and sealed in plastic bags to avoid light influence.

**3-2-3- Extraction Procedure**

One quarter (1/4) of sampled filter was soaked into 200 ml of ultrapure water (Milli-Q) in a 200 mL conical beaker wrapped the beaker with parafilm and aluminum foil keeping it in a shaker machine (multishaker MMS, EYELA) operating at 120rpm during 3h and filtered through syringe filter 0.45 μm PTFE (Akrodisk) and stored at ≈ 4°C until chemical analysis was performed. The pH was measured by a glass electrode pH meter (HM30S, TOA).

**3-2-4- Analytical Methods**

The concentrations of the major inorganic ions, dissolved organic carbon (DOC) and H$_2$O$_2$ were measured using ion chromatography (ICS –1600, Dionex), TOC analyzer (TOC-5000A, Shimadzu) and isocratic HPLC (LC-10Ai, Shimadzu), respectively. The total dissolved iron and other heavy metals were determined using inductively coupled plasma atomic emission spectrometry (Optima 3000, Perkin Elmer).

The initial concentration of H$_2$O$_2$ was determined according to the method described by Olasehinde *et al.* (2008) based on the reduction of H$_2$O$_2$ by ferrous iron (Fe$^{2+}$) in acid

solution to yield $^\bullet$OH which is scavenged by benzene to produce phenol and analyzed by isocratic HPLC (LC-10Ai, Shimadzu) with fluorescence detector ($\lambda_{Ex}$= 270 nm and $\lambda_{Em}$=298 nm).

### 3-2-5- OH radical measurement

$^\bullet$OH formation rate ($R_{OH}$) from the photo-Fenton reaction and total $R_{OH}$ were determined by HPLC-fluorescence detection (RF-10A, Shimadzu) following irradiation of the extracted sample using a solar simulator (Model 81160-100, Oriel Corp.) unit equipped with a 300 W Xenon lamp (ozone free, model 6258, Oriel Corp.). During photolysis, sample solutions were stirred by a magnetic stirrer covered with Teflon and maintained at a constant temperature of 20 °C using a circulator (RTE-111, NESLAB) and a chemical trap of photoformed $^\bullet$OH with benzene probe (1.2 mM) according to the methodology described by Faust and Allen (1993).

Therefore, $R_{OH}$ was then determined using the equation 11:

$$R_{OH} = (R_p/F_{b\text{-}OH}\ Y_p) \qquad (11)$$

where $R_p$ is the photochemical formation rate of phenol, $F_{b\text{-}OH}$ is the fraction of $^\bullet$OH that react with benzene, and $Y_p$ is the chemical yield of phenol from the reaction of $^\bullet$OH with the added benzene ($C_6H_6$).

Phenol ($C_6H_5OH$) was measured using isocratic HPLC with a pump (LC-10 Ai; Shimadzu), a $C_{18}$ column (LC-18 5 µm 4.6 mm i.d. x 250mm, Supelco or RP-18 GP 5µm 4.6 mm i.d. x 150 mm length, Kanto Kagaku) was used for separation and a fluorescence detector ($\lambda_{Ex}270/\lambda_{Em}$ 298 nm; RF-10A, Shimadzu). The mobile phase was acetonitrile and Milli-Q water [$CH_3CN:H_2O$ 60:40] (v/v) and the flow rate 1.0 mL min$^{-1}$.

The initial formation rate of phenol ($R_p$, M min$^{-1}$) during an illumination experiment was determined from the plot of phenol concentrations versus illumination time using a linear regression analysis.

The light intensity of the solar simulator was controlled measuring the photochemical degradation rate of 2-nitrobenzaldehyde (2-NB) by isocratic HPLC with UV detection of the absorbance wavelength set at 260 nm. The mobile phase and the flow rate were the same as for the determination of $^{\bullet}$OH. The degradation rate of 8μm 2-NB ($J_{2-NB}$) solution was normalized against a degradation rate of $J_{2-NB} = 0.00923$ s$^{-1}$ (Arakaki *et al.*, 1998).

The contribution of the photo-Fenton reaction was determined based on the difference between the $^{\bullet}$OH formation rates with and without the addition of deferoxamine mesylate (DFOM) (Sigma Aldrich, Japan). The addition of DFOM produces a stable and strong complex with Fe (III) that results in suppression of the photo-Fenton reaction (Nakatani *et al.* 2007). Next, 1 μM potassium trioxalate ferrate (III) is added to the solution of the WSG fraction with 0.5 μM $H_2O_2$ with and without 10 μM DFOM to determine the potential for generation of $^{\bullet}$OH from the photo-Fenton reaction (reactions 12 to14).

Fe (III)-(DOM) $_m$ + light $\rightarrow$ Fe (II)-DOM$_{m-1}$ + DOM$_{ox}^+$     (12)

Fe (OH) $^{2+}$ + light $\rightarrow$ Fe (II) + $^{\bullet}$OH       (13)

Fe (II) + $H_2O_2$ $\rightarrow$ Fe (III) + $^{\bullet}$OH + OH$^-$      (14)

The total dissolved iron was determined using inductively coupled plasma (ICP-AES) atomic emission spectrometry (Optima 7300-DV, Perkin Elmer).

### 3-2-6- Contribution of major sources of •OH (%)

The contributions of various sources to •OH photoproduction were estimated. The percent contributions ($fi$) from well-known •OH sources, such as $NO_3^-$, $NO_2^-$ and $H_2O_2$ to total •OH formation ($fi$ ($i$=$NO_3^-$, $NO_2^-$ and $H_2O_2$)) were calculated by the equation 17.

$$ fi = \frac{ki[Ci]}{R_{OH}total} \times 100(\%) \qquad (i=NO_3^-, NO_2^- \text{ and } H_2O_2) \qquad (17) $$

where $ki$ is the rate of •OH formation from nitrate ($k_{NO3-}$ = 2.43 x $10^{-7}$ $s^{-1}$), nitrite ($k_{NO2-}$ = 2.81 x$10^{-5}$ $s^{-1}$) and hydrogen peroxide ($k_{H2O2}$ = 3.52 x $10^{-6}$ $s^{-1}$), [$C_i$] is the concentration of each species and $R_{OHtotal}$ is the •OH photoproduction rate determined experimentally for the sample (Arakaki *et al.*, 1998; Nakatani *et al.*, 2001).

### 3-2-7- Fluorescence Properties

To estimate the unknown sources of •OH, the fluorescence matter (FM) was investigated based on the 3D-excitation emission matrix (EEM) spectrum obtained using a fluorescence spectrometer (F-4500, Hitachi, Ltd.). The samples were scanned at excitation wavelengths of 225-400 nm and emission wavelengths of 250-500 nm at intervals of 5 nm and a scanning speed of 1200 nm.min$^{-1}$ to obtain the overall characteristics. The samples were calibrated using 2.8 µg L$^{-1}$ of quinine sulfate dehydrated solution (Nacalai Tesque) as a standard for the total fluorescence intensity (FI), which corresponds to 25 quinine sulfate units (QSU).

### 3-2-8- Meteorological data

Meteorological parameters such as temperature (T), solar intensity (SI) and relative humidity (RH) were monitored by the automatic meteorological data acquisition system with the Global Positioning System (GPS) installed in the ship.

**3-3- Results and discussion**

**3-3-1- Chemical composition**

Table 3-2 shows the average and range concentration of chemical components in the water-extract of marine aerosols collected in Seto Inland Sea.

The abundance of chloride ($Cl^-$) and sodium ($Na^+$) was obvious, indicating predominance of sea salts particles in the aerosol samples collected. The mean concentration of $Cl^-$ and $Na^+$ are $36.3\pm51$ nmol m$^{-3}$ and $47.7\pm34$ nmol m$^{-3}$ respectively. $Cl^-$ represents 47.6% and $Na^+$ 52.6% of the total anions and cations respectively. Relatively lower percentages of sulfate ($SO_4^{2-}$) (32.1%) and nitrate ($NO_3^-$) (20.5%) in the present analysis (Table 3-2 and Figure 3-4) than those collected at Higashi-Hiroshima (*Chapter 2*) suggest the differences in chemical nature between the marine and land water-extract of aerosols. Nitrite ($NO_2^-$) was present in only 2 of the total 16 samples (mean of 1.4 nmol m$^{-3}$). The mean concentration of DOC was $7.0\pm6.6$ mg C m$^{-3}$ and the mean pH was $6.18\pm0.114$.

The sum of anions ($Cl^-$, $NO_3^-$, $SO_4^{2-}$, and $NO_2^-$) of each sample has been compared with that of cations ($Na^+$, $K^+$, $Ca^{2+}$, $Mg^{2+}$ and $NH_4^+$) to check the charge balance (Figure 3-5). The ratio of the sum of anions to that of cations averaged $0.72\pm0.37$ (R=0.83), indicating an existence of undetermined anions.

The Table 3-3 shows the sea-salts ratios calculated using $Na^+$ as reference element assuming all $Na^+$ to be of marine origin. The $Cl^-/Na^+$ ratios (0.64) determined in our samples were lower than the $Cl^-/Na^+$ ratio for seawater (1.79) reported by Millero (1996) indicating mixture of surface soil and sea salts (Pio and Lopes, 1998; Arakaki *et al.*, 2006).

The mean $SO_4^{2-}/Na^+$ ratio was 0.46 and ranged from 0.18 to 1.63 indicating no influence of soil dust or anthropogenic activities. However, the sample 5 showed higher ratio (1.63) than sea water (0.25) indicating that samples were possibly affected by anthropogenic

activities (including combustion of fossil fuels from the stack of the ship). The high $Ca^{2+}/Na^+$ ratios indicate the influence of soil dust/mineral aerosol. The good correlation between $Ca^{2+}$ and $NO_3^-$ (R=0.97) suggests its association with mineral aerosols (Müller *et al.*, 2001).

The Figure 3-6 shows individual aerosol composition at each sampling site. For each sample, we first analyzed the concentration at different sites and correlated the aerosol concentrations with the characterization of each site. This analysis can provide some insight to the dominant sources on each aerosol.

The moderate correlations between $Na^+$ and $Cl^-$ (R=0.61) or between $Na^+$ and other ions like $K^+$, $Ca^{2+}$ and $Mg^{2+}$ (R=0.62, R=0.99 and R=0.96 respectively) show the predominance of sea-salt aerosols in our samples (Table 3-4). The good correlations observed between $NH_4^+$ and $NO_3^-$ (R=0.95) and between $NH_4^+$ and $SO_4^{2-}$ (R= 0.90) suggest the existence form of ammonium sulfate, $(NH_4)_2SO_4$, and ammonium nitrate, $NH_4NO_3$. The existence of the $(NH_4)_2SO_4$ or $NH_4NO_3$ depends of the stability of the products of these ammonium compounds and depends on temperature and relative humidity as reported by Seinfeld (1986) and Parmar *et al.* (2001). $(NH_4)_2SO_4$ is most stable in most case while $NH_4NO_3$ is volatile and can be formed and remain stable in the particulate phase under high concentrations of $NH_3$ and $HNO_3$ and high humidity and temperature conditions (under RH 70 - 100%, temperature 30 - 42ºC, formation of $NH_4NO_3$ would be favored) (Parmar *et al.*, 2001). Therefore for our samples, due to lower relative humidity (mean of 66.9%) and temperature (mean of 26ºC) (Table 3-5), $(NH_4)_2SO_4$ must be the stable form.

### 3-3-2-•OH photoformation rate ($R_{OH}$) and contribution percentage (%)

All 16 samples were irradiated with a solar simulator to determine the •OH photoformation rate ($R_{OH}$). The concentrations of $NO_3^-$, $NO_2^-$, $H_2O_2$, FI, DOC and $R_{OH}$ are

listed in the Table 3.6. The range of the $R_{OH}$ determined in marine aerosol was from 0.019 to 0.14 nmol h$^{-1}$ m$^{-3}$ with the mean of 0.06±0.03 nmol h$^{-1}$m$^{-3}$(Figure 3-7).

The analysis of the ship speed combined to wind direction during the sample collection showed winds coming from the land affecting the samples and possibly explaining the variation of $R_{OH}$ in those some points (Table 3-7).

The Figure 3-8 shows the $R_{OH}$ variation for each aerosol sample. The highest $R_{OH}$ was observed in the samples 2, 9 and 11 corresponding to Aki-Nada ($R_{OH}$ = 0.114 nmol h$^{-1}$ m$^{-3}$), Osaka Bay ($R_{OH}$ = 0.096 nmol h$^{-1}$ m$^{-3}$) and Harima-Nada ($R_{OH}$ = 0.141 nmol h$^{-1}$ m$^{-3}$) respectively. These 3 samples are located near to the land (Figure 3-3) suggesting the influence of anthropogenic pollution as sources of $^{\bullet}$OH in those areas.

Specifically the samples 2 and 11 showed high concentrations of $NO_3^-$ and DOC. $NO_3^-$ contributes for 23.8% on the $^{\bullet}$OH production and the photo-Fenton 10.4% in the sample 2 while for the sample 11, $NO_3^-$ contributes for 12.1% and 7.4% for photo-Fenton. The $NO_2^-$ showed 93% of contribution in the sample 11. The unknown sources contribute for 46% and <1% in the samples 2 and 11 respectively. In order to clarify the sources of $^{\bullet}$OH, we estimated the contributions of various sources to $^{\bullet}$OH photoproduction. The contribution percentage from well-known $^{\bullet}$OH sources were calculated using the **equation 1** previously shown in the *Chapter 2*. The estimated contribution of $NO_3^-$ photolysis accounted for 9 – 47% (mean of 18.6%) of photochemically formed $^{\bullet}$OH in the marine aerosol samples (Table 3-6).

A good correlation between $R_{OHtotal}$ and concentration of $NO_3^-$ (R = 0.63; p<0.01) (Figure 3-9 (a)) suggests $NO_3^-$ as significant source of $^{\bullet}$OH generation in marine aerosols. $R_{OH}$ did not show correlations with concentration of DOC (R=0.27; p<0.01) and FI (sum of fluorescence intensities of the peaks A+B+C).

Nevertheless, the analysis of correlation between $R_{OHuknown}$ and the FI of each peak separately showed some relationship with $^\bullet$OH generation (discussed further). DOC and FI seemed to show an unclear correlation (R=0.49; p<0.01) (Figure 3.9c) although $R_{OHunknown}$ does not appear correlated with DOC concentrations (R= 0.22; p<0.01) (Figure 3.9d). Thus, due of the presence of organic compounds (DOC) detected in marine aerosol of the Seto Inland Sea, water-soluble organic compounds leads to the discussion and are thought as an important source of $^\bullet$OH. Mopper and Zhou (1990) suggested DOC was the major source of $^\bullet$OH in sea water.

The Table 3.8 shows the correlations between $R_{OH}$ and major sources of $^\bullet$OH combined. Non-correlation between the parameters was observed however some indicatives such as the presence of fluorescence properties in unknown fraction perhaps are involved to the photochemical production of $^\bullet$OH. Some significance in the correlation between $R_{OH}$ and FI (R=0.26, p<0.01) leads to the discussion that the presence of organic compounds has involvement as source of $^\bullet$OH.

In this study, an experiment was carried out to elucidate the sources of $^\bullet$OH. Photo-Fenton reaction was examined because this reaction is considered to be a major $^\bullet$OH source in both atmospheric aqueous phase and natural water (Nakatani et al. 2007). Dissolved iron species are common to exist in atmospheric aqueous phase (Kim et al. 2001, 2003). If water soluble gases meet with iron species in the aqueous phase photo-Fenton reaction may occur. To find potential sources of $^\bullet$OH in the atmospheric aqueous phase, known amount (excess) of iron (III) was added into the solution of the water-extract of marine aerosols and then the $R_{OH}$ of photo-Fenton reaction was determined by the method of Nakatani et al. (2007).

The Table 3.9 shows a comparison of the average contribution percentage of the major sources of $^\bullet$OH generation in WEA of marine aerosol obtained in this study and sea water.

In marine aerosols, $NO_3^-$ more contributed (18.6%) to the $^{\bullet}OH$ photoformation than $NO_2^-$, $H_2O_2$ and photo-Fenton reaction. However, unknown source(s) contribute for about 71%. In the sea water of Seto Inland Sea region, $NO_2^-$ (6.8%) and unknown (92.6%) sources showed to be most contributor of $^{\bullet}OH$ generation on surface water as reported by Takeda $et$ $al.$ (2004). Hydrogen peroxide was a less important source of $^{\bullet}OH$. The unknown sources are the most significant contributors of $^{\bullet}OH$ in WEA of marine aerosol suggesting that the unknown sources may significantly contribute to photoformation of $^{\bullet}OH$ as in the sea water.

The Table 3-10 summarizes the $R_{OH}$ obtained in this study and determined previously by other investigators. The $R_{OH}$ in water-extract of aerosols were found out lower (about 6 times) in this study compared to land aerosol, reported by Kondo $et$ $al.$ (2009); however the oxidation capacity of $^{\bullet}OH$ in our samples is comparable to coastal area of California and the remote area of Canada.

Alert in Canada is the northernmost permanently inhabited in the world. The low $R_{OH}$ determined in the snow packs have $NO_3^-$ as the significant source of $^{\bullet}OH$ generation (Wolff, 1995). However under some circumstances, photochemical reactions of particle-derived chromophores can be significant sources of $^{\bullet}OH$ and $H_2O_2$ in the Artic (Anastasio and Jordan, 2004). A study carried out in Okinawa presented 2 types of kinetics of the $^{\bullet}OH$ formation in the aerosol particles from the coastal area being possibly influenced by the Yellow Sand events (Arakaki $et$ $al.$, 2006). Since DOM represents one of the largest exchangeable organic reservoirs at the earth's surface and it has been pointed as a possible unknown source of $^{\bullet}OH$ generation for surface sea waters (Yamashita and Tanoue 2003).

**3-3-3- Fluorescence properties**

For most of the samples, two distinct wavelength of fluorescence excitation ($\lambda_{Ex}$) ranges and emission ($\lambda_{Em}$) ranges have been found ($\lambda_{Ex}$ 250-260 and $\lambda_{Em}$ 380-480nm) within the

scanned wavelength ($\lambda_{Ex}$ = 225-400nm and $\lambda_{Em}$=250-500nm) which are characteristics of Humic-Like Substances (HULIS) (Coble *et al.*, 1990; Coble, 1996; Parlanti *et al.*, 2000; Zepp *et al.* 2004; Graber and Rudich, 2006).

Previous studies found that dissolved organic compounds had three distinctive peaks (A, B and C) in the 3D-EES obtained from sea water samples. In our study case, three peaks of fluorescence were observed in the contour plots spectra of marine aerosols (Figure 3.10).

A highest peak was observed at $\lambda_{Ex/Em}$=240–270/350–450nm (peak A), with the mean of 43.6±19.7 QSU or flu, the second peak was observed at $\lambda_{Ex/Em}$= 305–320/395–420 nm (peak B), with the mean of 27.2±16 QSU indicating the presence of HULIS in the marine aerosols collected in the Seto Inland Sea (Table 3-11). A third peak, peak C, at $\lambda_{Ex/Em}$ = 260-285/305-345 nm was found in 12 samples with a mean of 23.6±8.6 QSU. Nakajima *et al.* (2008) also reported that the presence of those two peaks in the aerosol of Okinawa. Although not exactly same wavelengths as Nakajima *et al.*, 2008 reported for the samples collected in Okinawa, aromatic amines such as tryptophan and proteins might exist in our samples.

The presence of the peaks A and B were confirmed in 15 aerosol samples and 12 showed the peak C. No correlations between $R_{OHunknown}$ and FI (A+B+C) were observed however; between $R_{OHunknown}$ and the peaks A and B and C (separately) some relationship was detected (Table 3-8).

The correlations between $R_{OHuknown}$ and FI of the peaks A, B and C were found in this study (R=0.21, R=0.21 and R=0.50; p<0.01 respectively) (Figure 3-11a-c). Although no clear correlations were observed between the $R_{OHunknown}$ and peaks A and B, the peak C, the presence of fluorescence properties possibly indicates that organic compounds are perhaps related with generation of $^{\bullet}OH$.

The results of the fluorescence properties suggested the presence of carbonaceous compounds and may be related with $^{\bullet}$OH generation in the water-extract of marine aerosols. As Mopper and Zhou (1990), Zhou and Mopper, 1990 and Vaughan and Blough, 1998 had reported, the photolysis of DOM has been believed to be a source of $^{\bullet}$OH formation in natural waters. However, further researches are needed to better understand the various and complex mechanisms involving the $^{\bullet}$OH formation from the photolysis of DOM in the water-extracts of marine aerosol.

Therefore, the fluorescence technique used for characterization of carbonaceous compounds in our samples provided information about the possible presence of HULIS substances and tryptophan. Mostafa *et al.* (2005) reported in their photo irradiation experiment the changes (shifts) in the fluorescence peak wavelengths of standard Suwannee River Fulvic Acid (SRFA) with increasing solar simulator irradiation time (30 min) while fluorescence intensity of SRFA was no change during the irradiation, which phenomena was explained by low photosensitivity of the SRFA and its high molecular size and complex structures (Malcom, 1985; Senesi, 1990, Münster *et al.,* 1999).

Reactions involving the photolysis of DOM have been believed as a major source of $^{\bullet}$OH formation in natural waters (river and sea waters) (Vaughan and Blough, 1998; Mopper and Zhou, 1990; Anastasio and Newberg, 2007). Thus, for this study there is a hypothesis that DOM may be the most significant source of $^{\bullet}$OH production in the marine aerosols.

**3-4- Conclusions**

This study determined the $^{\bullet}$OH photoformation rate, chemical composition, sources and major contributors of $^{\bullet}$OH in the water-extract of marine aerosols. In the Seto Inland Sea region, as a coastal sea, sea salts were the major contributing source of aerosol particles. Sea

salts such as $Na^+$ and $Cl^-$ were observed most abundant species in the marine aerosol. The $SO_4^{2-}/Na^+$ ratio (0.46) indicates that samples were possibly affected by anthropogenic activities. The low $R_{OH}$ observed in the samples may reflect small amount of $^\bullet OH$ generation sources and oxidation capacities in coastal atmosphere. $NO_3^-$ accounted for a significant contribution percentage (18.6%) of $^\bullet OH$ generation in marine aerosols. The results also revealed that unknown sources were the most important sources of $^\bullet OH$ (74%) suggesting similar mechanisms of $^\bullet OH$ formation as sea water. The unknown source related to the dissolved organic compounds showed no clear correlation between the FI and DOC concentrations. However previous studies had reported a mechanism involving the photolysis of DOM occurring in the natural and sea waters have been suggested to be the major source of $^\bullet OH$ formation in the water-extract of marine aerosols.

**References**

Allen, J.M., Lucas, S., Allen, S.K., 1996. Formation of hydroxyl radical in illuminated surface waters contaminated with acidic mine drainage. Environmental Toxicology and Chemistry, 15, 107-113.

Anastasio, C., Faust, B.C., Allen, J.M., 1994. Aqueous phase photochemical formation of hydrogen peroxide in authentic cloud waters. Journal of Geophysical Research 99 (D4), 8231- 8248.

Anastasio, C. and McGregor, K.G., 2001. Chemistry of fog waters in California's Central Valley: 1. In situ photoformation of hydroxyl radical and singlet molecular oxygen. Atmospheric Environment 35, 1079-1089.

Anastasio, C. and Newberg, J.T., 2007. Sources and sinks of hydroxyl radical in sea-salt particles. Journal of Geophysical Research 112, 13.

Anastasio, C. and Jordan, A.L., 2004. Photoformation of hydroxyl radical and hydrogen peroxide in aerosol particle from Alert, Nunavut: implications for aerosol and snowpack chemistry in the Artic. Atmospheric Environment 38, 1153-1166.

Arakaki, T. and Faust, B.C., 1998. Sources, sinks, and mechanisms of hydroxyl radical photoproduction and consumption in authentic acidic continental cloud waters from Whiteface in Mountain, New York: the role of the Fe(r) (r = II, III) photochemical cycle. Journal of Geophysical Research 103 (D3), 3487-3504.

Arakaki, T., Miyake, T., Shibata, M. and Sakugawa, H., 1998. Measurement of photochemically formed hydroxyl radical in rain and dew waters. The Chemical Society of Japan, 9, 619-625 (in Japanese).

Arakaki, T., Kuroki, Y., Okada, K., Nakama, Y., Ikota, H., Higuchi, T., Uehara, M., Tanahara, A., 2006. Chemical composition of photochemical formation of hydroxyl radical in aqueous extracts of aerosol particles collected in Okinawa, Japan. Atmospheric Environment 40, 4764-4774.

Chen, G., Huey, L.G., Trainer, M., 2005. An investigation of the chemistry of ship emission plumes during ITCT 2002. Journal of Geophysical Research D, vol. 110, no.10, Article ID D10S90, 15 pages.

Coble, P.G., Green, S.A., Blough, N.V., Gagosian, R.B., 1990. Characterization of dissolved organic matter in the Black Sea by fluorescence spectroscopy. Nature 348 (6300), 432-435.

Coble, P.G., 1996. Characterization of marine and terrestrial DOM in sea water using excitation-emission matrix spectroscopy. Marine Chemistry 51, 325-346.

Duce, R.A., 2005. In: Oliver, J.E. (Ed.), Aerosols, Encyclopedia of World Climates. Kluwer, Dordrecht, pp. 4–6.

Faust, B.C. and Allen, J.M., 1993. Aqueous-phase photochemical formation of hydroxyl radical in authentic cloudwaters and fogwaters. Environmental Science and Technology 27, 1221-1224.

Faust, B.C., Anastasio, C., Allen, J.M., Arakaki, T., 1993. Aqueous-phase photochemical formation of peroxides in authentic cloud and fog waters. Science 260, 73-75.

Graber, E. R. and Rudich, Y., 2006. Atmospheric HULIS: How humic-like are they? A comprehensive and critical review. Atmospheric Chemistry and Physics 6, 729-753.

Huang, J., Minnis, O., B. Chen, 2008. Long-range transport and vertical structure of Asian dust from CALIPSO and surface measurements during PACDEX. Journal of Geophysical Research D, vol. 113, no.23, Article ID D23212.

Keene, W.C., Maring, H., Maben, J.R., Kieber, D.J., Pszenny, A.A.P., Dahl, E.E., Izaguirree, M.A., Davis, A.J., Long, M.S., Zhou, X., Smoydzin, L., Sander, R., 2007. Chemical and physical characteristics of nascent aerosols produced by bursting bubbles at a model air-sea interface. Journal of Geophysical Research 112, doi: 10.1029/2007JD008464.

Kim, D.H., Takeda, K., Sakugawa, H., Lee, J.S., 2001. The determination of dissolved total Fe by flow injection analysis in environmental samples. Analytical Science & Technology Vol. 14 (6), 510-515.

Kim, D.H., Takeda, K., Sakugawa, H., Lee, J.S., 2003. The photochemical reactions of iron species in rain and snow in Higashi-Hiroshima, Japan. Analytical Science & Technology Vol. 16 (6), 466-474.

Kondo, H., Chiwa, M., Sakugawa, H., 2009. Photochemical formation and scavenging mechanisms of hydroxyl radical in water-extracts of atmospheric aerosol collected in Higashi-Hiroshima, Japan. Geochemistry 43, 15-25 (in Japanese).

Malcolm, R. L., 1985. Geochemistry of stream fulvic and humic substances. Humic Substances in Soil, Sediment, and Water: Geochemistry, Isolation and Characterization (Aiken, G. R., McKnight, D. M., Wershaw, R. L. and MacCarthy, P., eds.), 181–209, Wiley.

Millero, F.L., 1996. Chemical Oceanography. CRC Press, Boca Raton, Tokyo.

Mopper, K., and Zhou, X., 1990. Hydroxyl radical photoproduction in the sea and its potential impact on marine processes. Science, 250, 661-664.

Mostofa, K. M. G., Honda, Y. and Sakugawa, H., 2005. Dynamics and optical nature of fluorescent dissolved organic matter in river waters in Hiroshima prefecture, Japan. Geochem. J. **39**, 257–271.

Muller, D., Franke, K., Wagner, F., Althausen, D., Ansmannm A., Heintzenberg, J., 2001. Vertical profiling over the tropical Indian Ocean with sex-wavelength lidar: 1, seasonal cycle. Journal of Geophysical Research 106, 28567-28575.

Münster, U., Salonen, K. and Tulonen, T., 1999. Decomposition. Limnology of Humic Waters (Keskitalo, J. and Eloranta, P., eds.), 225–263, Backhuy Publishers.

Nakajima, H., Okada, K., Kuroki, Y., Nakama, Y., Handa, D., Arakaki, T., Tanahara, A., 2008. Photochemical formation of peroxides and fluorescence characteristics of the water-soluble fraction of bulk aerosols collected in Okinawa, Japan. Atmospheric Environment 42, 3046-3058.

Nakatani, N., Miyake T., Chiwa, M., Hashimoto, N., Arakaki, T. and Sakugawa, H., 2001. Photochemical formation of OH radicals in dew formed on the pine needles at Mt. Gokurakuji. Water, Air and Soil Pollution 130: 397-402.

Nakatani, N., Ueda, M., Shindo, H., Takeda, K., and Sakugawa, H., 2007. Contribution of the Photo-Fenton reaction to hydroxyl radical formation rates in river and rain water samples. Analytical Sciences, 23, 1137-1142.

O'Dowd, C. D. and de Leeuw, G., 2007. Marine aerosol production: a review of the current knowledge, Philosophical Transactions of the Royal Society, 365, 2007–2043.

Olasehinde, E.F., Makino, S., Kondo, H., Takeda, K., Sakugawa, H., 2008. Application of Fenton reaction for nanomolar determination of hydrogen peroxide in seawater. Analytica Chimica Acta, 627, 270-276.

Parmar, R.S., Satsangi, G.S., Kumari, M., Lakhani, A., Srivastava, S.S., Prakash, S., 2001. Study of size distribution of atmospheric aerosol at Agra. Atmospheric Environment 35, 693-702.

Parlanti, E., Worz, K., Geoffroy, L.M., 2000. Dissolved organic matter fluorescence spectroscopy as a toll to estimate biological activity in a coastal zone submitted to anthropogenic inputs. Organic Geochemistry 31 (12), 1765-1781.

Pio, C.A. and Lopes, D.A., 1998. Chlorine loss from marine aerosol in a coastal atmosphere. Journal of Geophysical Research 103 (D19), 25263-25272.

Qian, J., Mopper, K., Kieber, D.J., 2001. Photochemical production of the hydroxyl radical in Antarctic waters. Deep-Sea Res. Pt. I 48, 741-759.

Seinfeld, J.H., 1986. Atmospheric Chemistry and Physics of Air Pollution. Willey-Interscience, New York, pp. 378-382.

Senesi, N., 1990 Molecular and quantitative aspects of the chemistry of fulvic acid and its interactions with metal ions and organic chemicals. Part II. The fluorescence spectroscopy approach. Anal. Chim. Acta 232, 77–106.

Takeda, K., Tadedoi, H., Yamaji, S., Ohta, K., Sakugawa, H., 2004. Determination of hydroxyl radical photoproduction rates in natural waters. Analytical Sciences 20, 153-159.

Vaughan, P.P. and Blough, N.V., 1998. Photochemical formation of hydroxyl radicals by constituents of natural waters. Environmental Science and Technology 32, 2947-2953.

Yamashita, Y., Tanoue, E., 2003. Chemical characterization of protein-like fluorophores in DOM in relation to aromatic amino acids. Marine chemistry 82, 255-271.

Yanagi, T. and Okaichi, T., 1997. Seto Inland Sea – Historical background. Sustainable development in the Seto Inland Sea, Japan – From the viewpoint of fisheries, Eds. T. Okaichi and T. Yanagi, pp. 9-14.

Zepp, R. G., Sheldon, W.M., Moran, M.A., 2004. Dissolved organic fluorophores in southeastern US coastal waters; correction method for eliminating Rayleigh and Raman scattering peaks in excitation-emission matrices. Marine Chemistry 89 (1-4), 15-36.

Zhou, X. and Mopper, K., 1990. Apparent partition coefficients of 15 carbonyl compounds between air and seawater and between air and freshwater: Implications for air-sea exchange. Environ. Sci. Technol., 24: 1864-1869.

White, E.M., Vaughan, P.P., Zepp, R.G., 2003. Role of the photo-Fenton reaction in the production of hydroxyl radicals and photobleaching of colored dissolved organic matter in a coastal river of the southern United States. Aquatic Science 65, 402-414.

Wolff, E. W., 1995. Nitrate in polar ice. In: Delmas, R.J. (Ed.), Ice core studies of global biogeochemical cycles. Springer, Berlin, 1-3.
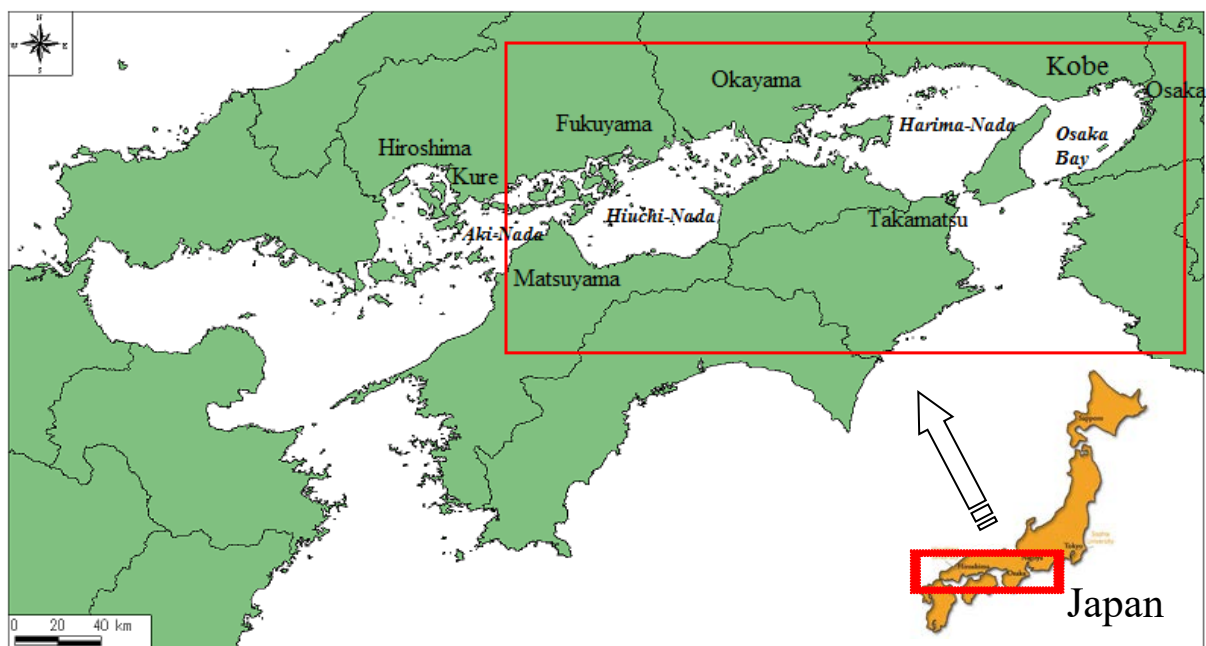
**Figure 3-1.** Map of sampling area: Seto Inland Sea region, in Japan



**Figure 3-2.** High Volume Air Sampler set up on the deck of Toyoshio Maru

**Table 3-1.** Aerosol sampling schedule: Seto Inland Sea and Osaka Bay

| Sample | Day | Time | Coordinates | Area |
|--------|-----|------|-------------|------|
| 1 | 2010.9.13 | 10:00-11:16 | 34°06.07' N; 132° 38.06' E | Aki Nada |
| 2 | 2010.9.13 | 11:45-12:15 | 34°06.43' N; 132° 44.55' E | Aki Nada |
| 3 | 2010.9.13 | 12:30-14:40 | 34°08.08' N; 133° 09.94' E | Hiuchi Nada |
| 4 | 2010.9.13 | 15:00-16:20 | 34°12.98' N; 133° 24.96' E | Hiuchi Nada |
| 5 | 2010.9.13 | 16:37-19:31 | 34°25.00' N; 133° 59.95' E | Harima Nada |
| 6 | 2010.9.14 | 7:25-9:25 | 34°36.94' N; 135° 00.82' E | Harima Nada |
| 7 | 2010.9.14 | 9:30-11:30 | 34°27.94' N; 135° 07.77' E | Osaka Bay |
| 8 | 2010.9.14 | 11:30-13:30 | 34°37.88' N; 135° 17.05' E | Osaka Bay |
| 9 | 2010.9.14 | 13:33-15:03 | 34°38.06'N 135°11.17'E | Osaka Bay |
| 10 | 2010.9.15 | 8:00-10:30 | 34°36.64' N; 134° 44.88' E | Osaka Bay |
| 11 | 2010.9.15 | 10:55-11:32 | 34°31.23' N; 134° 36.38' E | Harima Nada |
| 12 | 2010.9.15 | 11:50-13:00 | 34°22.96' N; 134° 24.98' E | Harima Nada |
| 13 | 2010.9.15 | 13:20-17:20 | 34°19.08' N; 133° 37.24' E | Harima Nada |
| 14 | 2010.9.15 | 17:40-19:25 | 34°20.26' N; 133° 13.87' E | Hiuchi Nada |
| 15 | 2010.9.16 | 8:00-10:00 | 34°17.63' N; 132° 52.48' E | Hiuchi Nada |
| 16 | 2010.9.16 | 10:00-11:50 | 34°11.66'N; 132°32.24'E | Aki Nada |
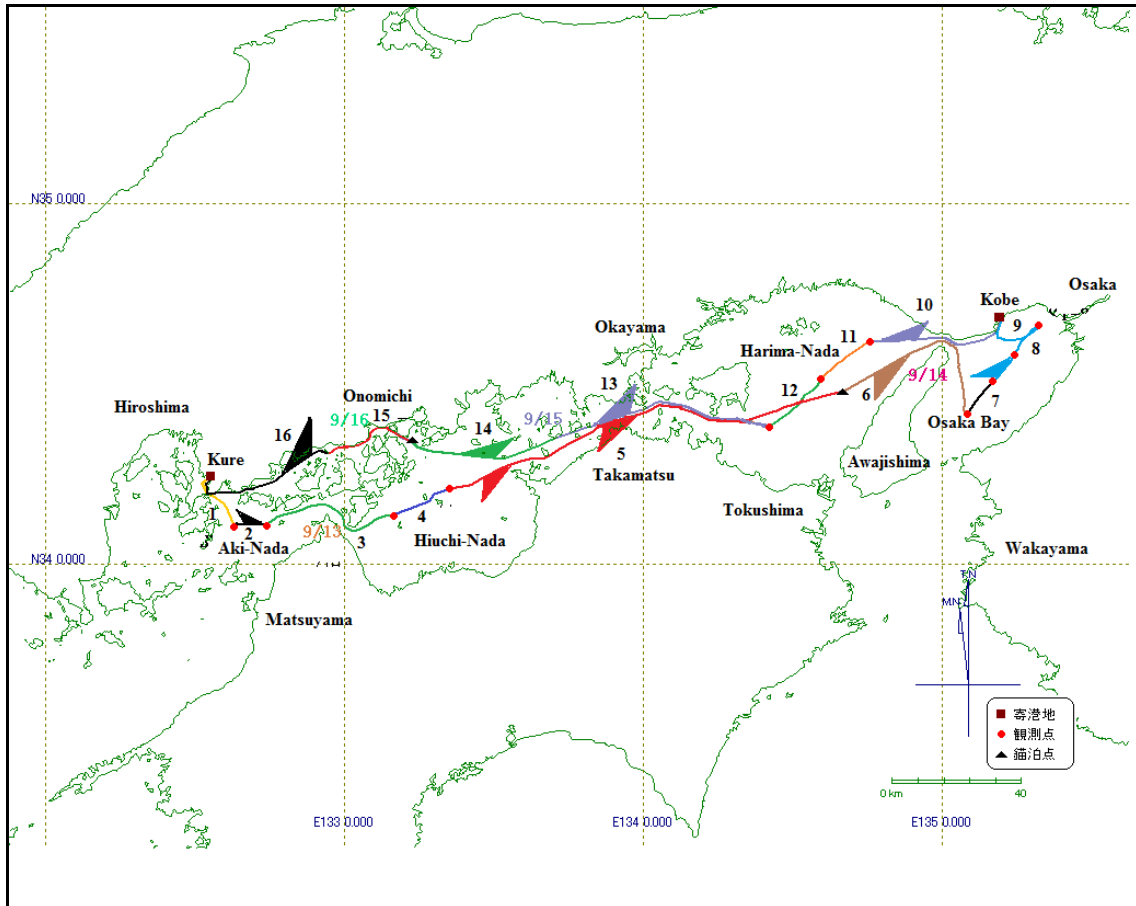
**Figure 3-3.** Map of cruise trajectory through the Seto Inland Sea by the Toyoshio-Maru, September 13<sup>th</sup> – 16<sup>th</sup>, 2010

**Table 3-2.** Chemical composition of water-extract of marine aerosols

|  | (mean± SD) | Range |
|---|---|---|
| $Cl^-$ | 36.3±51 | 0.02 - 160 |
| $NO_3^-$ | 11±6.8 | 5.0 – 32.6 |
| $NO_2^-$ | 1.4±0.1 | ND-1.5 |
| $SO_4^{2-}$ | 18.1±11 | 7.8 – 48.4 |
| (nss)-$SO_4^{2-}$ | 6.2±7.1 | ND – 22.5 |
| $NH_4^+$ | 3.9±2.2 | 1.6 – 10.4 |
| $Na^+$ | 47.7±34 | 16.1 – 157 |
| $K^+$ | 15.5±21 | 2.3 – 87 |
| $Ca^{2+}$ | 13.6±10 | 4.84–46 |
| $Mg^{2+}$ | 9.9±6.9 | 3.2 – 30.9 |
| Fe | 0.15±0.09 | ND – 0.321 |
| DOC* | 7.05±6.6 | 0.8 – 29.4 |
| $H_2O_2$ | 0.51±0.6 | ND– 0.91 |
| pH | 6.18±0.114 | 5.89-6.32 |

*Note:* Mean indicates arithmetic mean.     SD: Standard Deviation     ND: not detectable
*mg C m$^{-3}$                               Unit: nmol.m$^{-3}$
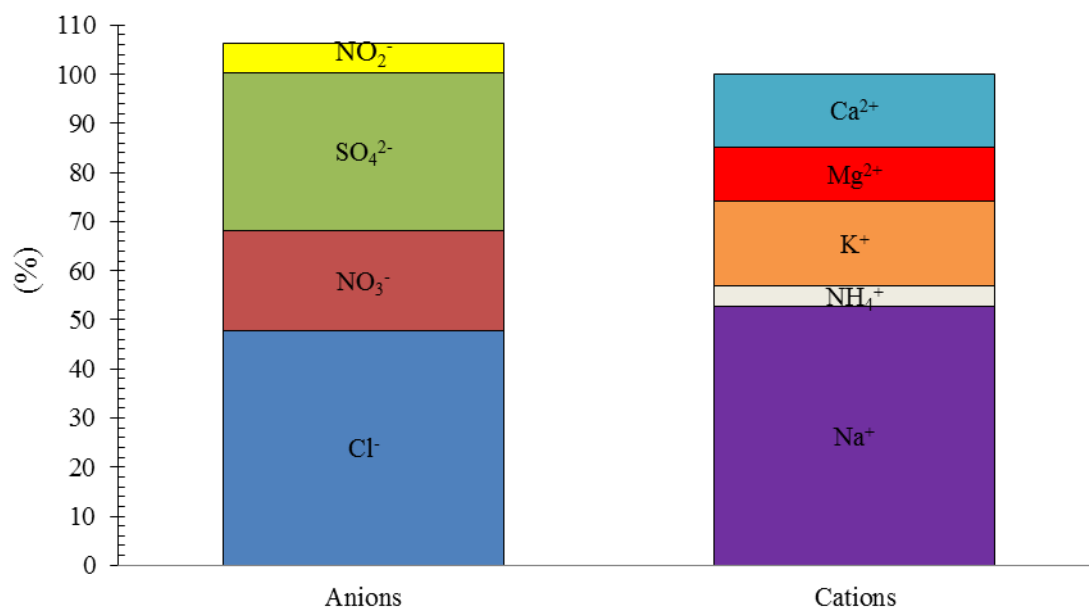
**Figure 3-4.** Percentage distribution of major cations and anions.
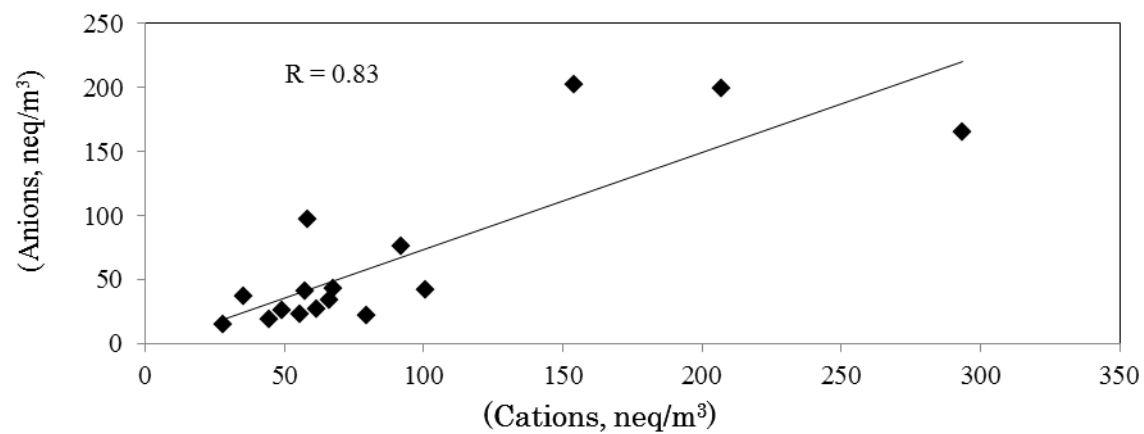


**Figure 3-5.** Charge balance of ions in water-extract of marine aerosols

**Table 3-3.** Mass-based ratio of chemical constituents relative to $Na^+$

| Sample | $Cl^-/Na^+$ | $SO_4^{2-}/Na^+$ | $Mg^{2+}/Na^+$ | $Ca^{2+}/Na^+$ |
|--------|-------------|------------------|----------------|----------------|
| 1 | 1.87 | 0.41 | 0.17 | 0.25 |
| 2 | 0.53 | 0.31 | 0.19 | 0.29 |
| 3 | 0.30 | 0.72 | 0.19 | 0.29 |
| 4 | 1.0 | 0.70 | 0.25 | 0.28 |
| 5 | 0.18 | 1.63 | 0.29 | 0.32 |
| 6 | 2.4 | 0.34 | 0.20 | 0.28 |
| 7 | 0.26 | 0.27 | 0.19 | 0.32 |
| 8 | 0.36 | 0.29 | 0.19 | 0.29 |
| 9 | 0.12 | 0.18 | 0.20 | 0.29 |
| 10 | 0.14 | 0.31 | 0.29 | 0.29 |
| 11 | 1.84 | 0.24 | 0.23 | 0.31 |
| 12 | 0.24 | 0.24 | 0.30 | 0.3 |
| 13 | - | 0.54 | 0.20 | 0.3 |
| 14 | - | 0.30 | 0.15 | 0.19 |
| 15 | 0.33 | 0.41 | 0.14 | 0.23 |
| 16 | - | 0.52 | 0.21 | 0.27 |
| | | | | |
| Mean | 0.64 | 0.46 | 0.21 | 0.28 |
| STD | 0.76 | 0.33 | 0.05 | 0.03 |
| | | | | |
| Sea water | 1.79 | 0.25 | 0.12 | 0.04 |

*Note: - : not available*
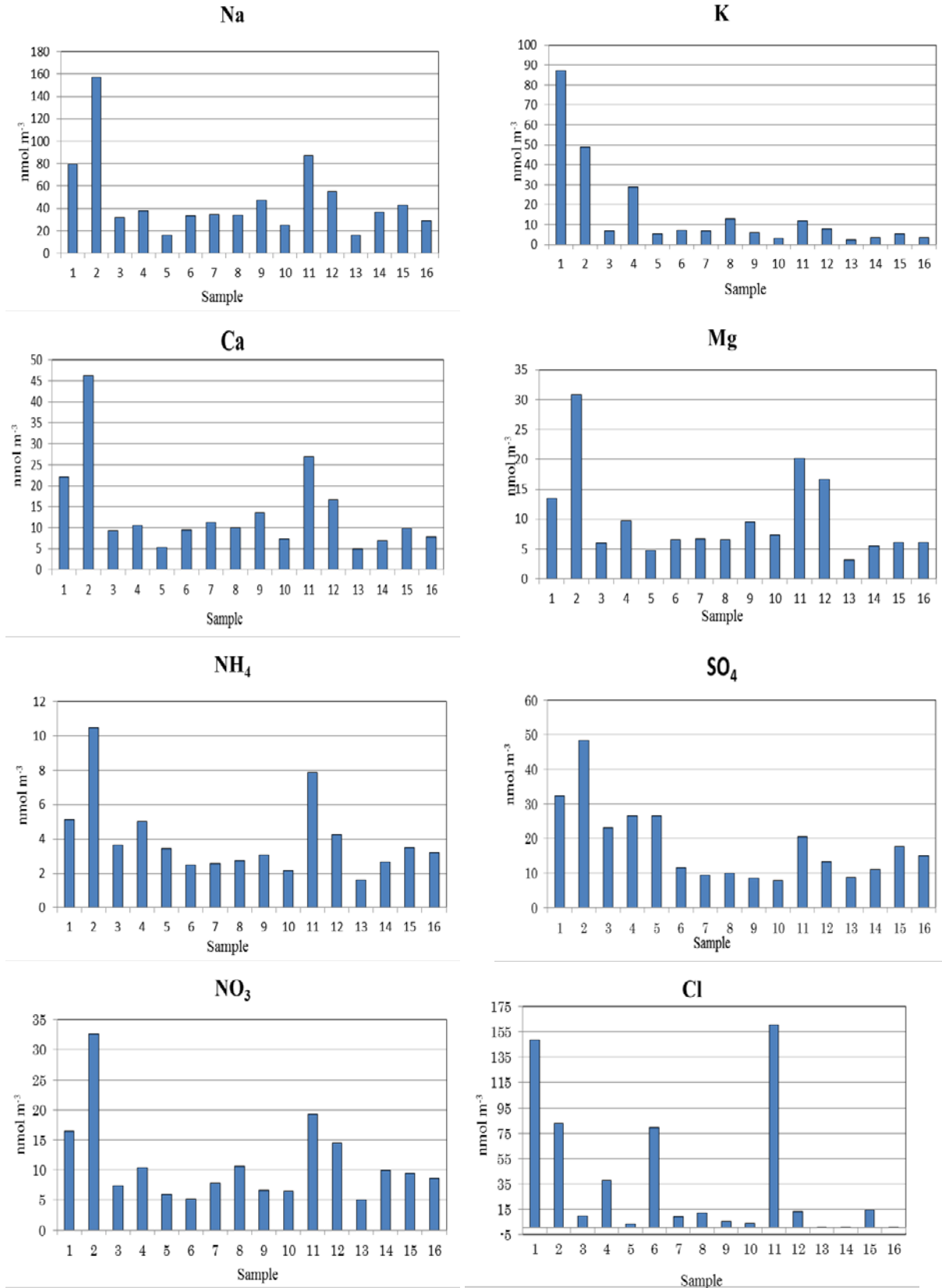
**Figure 3-6.** Concentrations of Cl⁻, NO₃⁻, SO₄²⁻, Na⁺, NH₄⁺, K⁺ and Mg²⁺ measured in each marine aerosol samples.

**Table 3-4.** Multi-correlation coefficients (R) involving major ions determined in marine aerosols

|  | $Na^+$ | $K^+$ | $Ca^{2+}$ | $Mg^{2+}$ | $NH_4^+$ |
|---|---|---|---|---|---|
| $Na^+$ | 1 | 0.62 | 0.99 | 0.96 | 0.93 |
| $Cl^-$ | 0.61 | 0.67 | 0.65 | 0.61 | 0.66 |
| $NO_3^-$ | 0.97 | 0.60 | 0.96 | 0.95 | 0.94 |
| $SO_4^{2-}$ | 0.82 | 0.71 | 0.74 | 0.69 | 0.93 |

**Table 3-5.** Temperature, relative humidity and solar intensity during the cruise (Feb. 13th-16th , 2010

| Sample | Temperature, ºC | Relative Humidity, % | Solar intensity, MJ/m² |
|---|---|---|---|
| 1 | 25 | 74.8 | 11.6 |
| 2 | 24.3 | 78 | 20.8 |
| 3 | 25.9 | 65.5 | 22.4 |
| 4 | 27.8 | 60.3 | 27.1 |
| 5 | 27.1 | 69.6 | 3.61 |
| 6 | 26.1 | 65.6 | 26 |
| 7 | 26.4 | 64 | 35.5 |
| 8 | 27.7 | 60.6 | 17.1 |
| 9 | 27.1 | 62 | 11.2 |
| 10 | 26 | 63.6 | 21 |
| 11 | 26.3 | 65.7 | 16 |
| 12 | 26.1 | 66.8 | 20.5 |
| 13 | 26.5 | 63.1 | 4.6 |
| 14 | 25.96 | 69.6 | 0.08 |
| 15 | 23.1 | 74.5 | 34.2 |
| 16 | 25 | 67.5 | 49.2 |
| Mean | 26.02 | 66.95 | 20.06 |

**Table 3-6.** The contribution of major sources of $^{\bullet}OH$ to the marine aerosols collected in the Seto Inland Sea, Japan.

| n | Concentration, nmol m$^{-3}$ | | | | | | Contribution$^a$, % | | | | | |
|---|---|---|---|---|---|---|---|---|---|---|---|---|
| | $R_{OH}{}^*$ | $NO_2{}^-$ | $NO_3{}^-$ | $H_2O_2$ | FI$^{**}$ | $^{***}DOC$ | $f_{NO2^-}$ | $f_{NO3^-}$ | $f_{H2O2}$ | $f_{Photo\text{-}Fenton}{}^b$ | $f_{Unknown}{}^c$ | $R_{OH\ unknown}{}^d$ |
| 1 | 0.05 | 1.5 | 27.6 | 0.4 | 48.1 | 12.3 | ND | 27.6 | 9.75 | *4.22* | - | - |
| 2 | 0.12 | ND | 23.8 | 1.36 | 19.8 | 0.8 | ND | 24 | 14.3 | 10.4 | 45.9 | 0.055 |
| 3 | 0.02 | ND | 26.6 | ND | 55.4 | 5.2 | ND | 26.6 | ND | 1.19 | 65.6 | 0.016 |
| 4 | 0.04 | ND | 20.7 | ND | 100.7 | 5.3 | ND | 20.7 | ND | 3.36 | 70.2 | 0.031 |
| 5 | 0.07 | ND | 7.48 | ND | 173.3 | 8.7 | ND | 7.5 | ND | 1.68 | 89.2 | 0.062 |
| 6 | 0.04 | ND | 12.6 | ND | 66.2 | 3.8 | ND | 12.6 | ND | 3.42 | 80.5 | 0.029 |
| 7 | 0.02 | ND | 36.4 | ND | 173.3 | 5.0 | ND | 36.4 | ND | 2.0 | 52.2 | 0.010 |
| 8 | 0.02 | ND | 40.5 | ND | 66.2 | 5.8 | ND | 40.5 | ND | 2.12 | 50.1 | 0.011 |
| 9 | 0.10 | ND | 5.86 | ND | 59.4 | 2.7 | ND | 5.8 | ND | 1.46 | 90.3 | 0.089 |
| 10 | 0.04 | ND | 13.2 | ND | 60.2 | 7.4 | ND | 13.2 | ND | 2.36 | 81.1 | 0.035 |
| 11 | 0.14 | 1.3 | 12.1 | ND | 42.4 | 1.5 | 93.9 | 12.1 | ND | 7.4 | - | - |
| 12 | 0.06 | ND | 22.0 | ND | 71.8 | 2.1 | ND | 22 | ND | 21 | 51.9 | 0.030 |
| 13 | 0.05 | ND | 8.68 | ND | 41.2 | 29.4 | ND | 8.7 | ND | 4.3 | 85.4 | 0.043 |
| 14 | 0.07 | ND | 13.2 | ND | 43.3 | 7.5 | ND | 13.2 | ND | 5.4 | 79.3 | 0.052 |
| 15 | 0.05 | ND | 15.3 | ND | 112.9 | 8.2 | ND | 15.3 | ND | 6.21 | 75.4 | 0.041 |
| 16 | 0.06 | ND | 12.4 | ND | 81.4 | 7.1 | ND | 12.4 | ND | 5.5 | 79.3 | 0.048 |
| Mean | 0.06 | 1.4 | 18.6 | 0.88 | 76 | 7.05 | - | 18.6 | 12 | 5.05 | 71 | 0.03 |
| SD | 0.03 | 0.14 | 9.85 | 0.5 | 43 | 6.7 | - | 9.8 | 2.3 | 4.7 | 14.8 | 0.05 |

*Notes:* $^*$R$_{OH}$: nmol h$^{-1}$ m$^{-3}$  $^{**}$QSU: Quinine Sulfate Unit  $^{***}$mg C m$^{-3}$  - : not available  ND: not detected

$^a f_i = [k_i[C_i]/R_{OHtotal}] \times 100$ (%)  $^b$Generation potential of $^{\bullet}OH$ from photo-Fenton reaction

$^c f_{unknown} = 100 - (f_{NO3^-} + f_{NO2^-} + f_{H2O2})$ (%)  $^d R_{OHunknown} = (R_{OH} \times f_{unknown})/100$

**Table 3-7.** Wind direction (WD), Direction (D), ship speed (SS) in nautical miles and (SS')
in m/min.

| Sample | WD | D | SS | SS' |
|--------|--------|-----|------|-----|
| #1 | 213.1 | SWW | 9.2 | 4.9 |
| #2 | 192.3 | SWW | 10 | 5.4 |
| #3 | 237.1 | SSW | 11.1 | 6 |
| #4 | 265.9 | SSW | 9.9 | 5.3 |
| #5 | 256.2 | SSW | 10.8 | 5.8 |
| #6 | 294.09 | SSE | 9.44 | 5.1 |
| #7 | 292.3 | SSE | 8.22 | 4.4 |
| #8 | 258.8 | SSW | 6.3 | 3.4 |
| #9 | 322.5 | SEE | 8.33 | 4.5 |
| #10 | 252.1 | SSW | 9.9 | 5.3 |
| #11 | 176.8 | NWW | 10.9 | 5.9 |
| #12 | 317.8 | SEE | 10.6 | 5.7 |
| #13 | 261.2 | SSW | 10.3 | 5.6 |
| #14 | 294.3 | SSE | 9.7 | 5.2 |
| #15 | 248.6 | SSW | 10.2 | 5.5 |
| #16 | 193.4 | SWW | 10.1 | 5.5 |
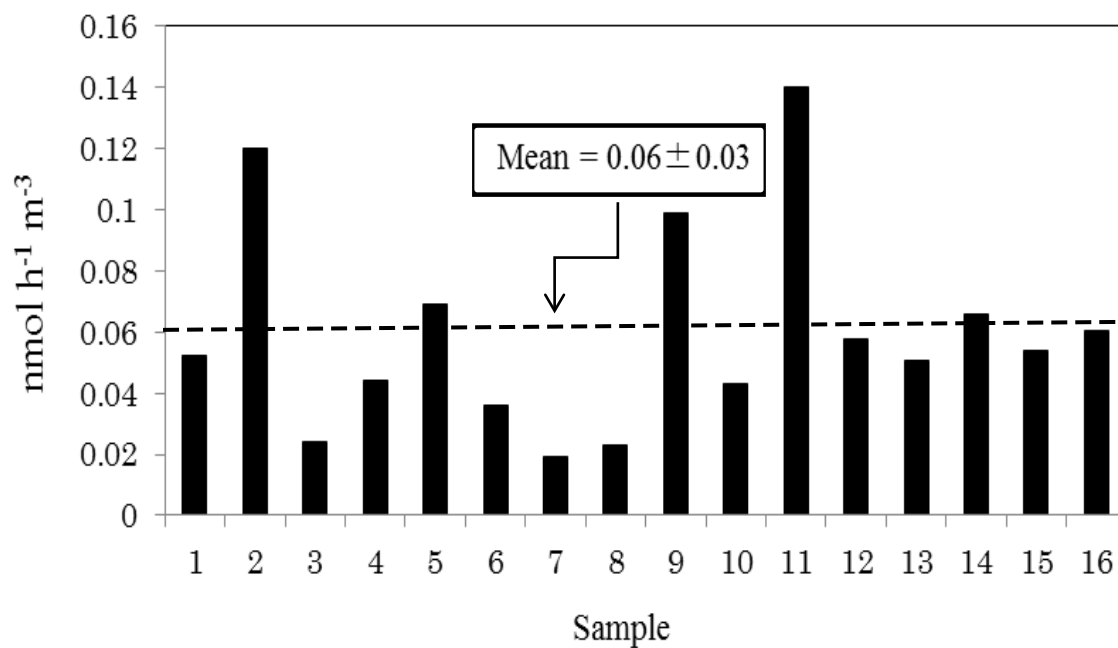
**Figure 3-7.** •OH photoformation rate variation in Seto Inland Sea region
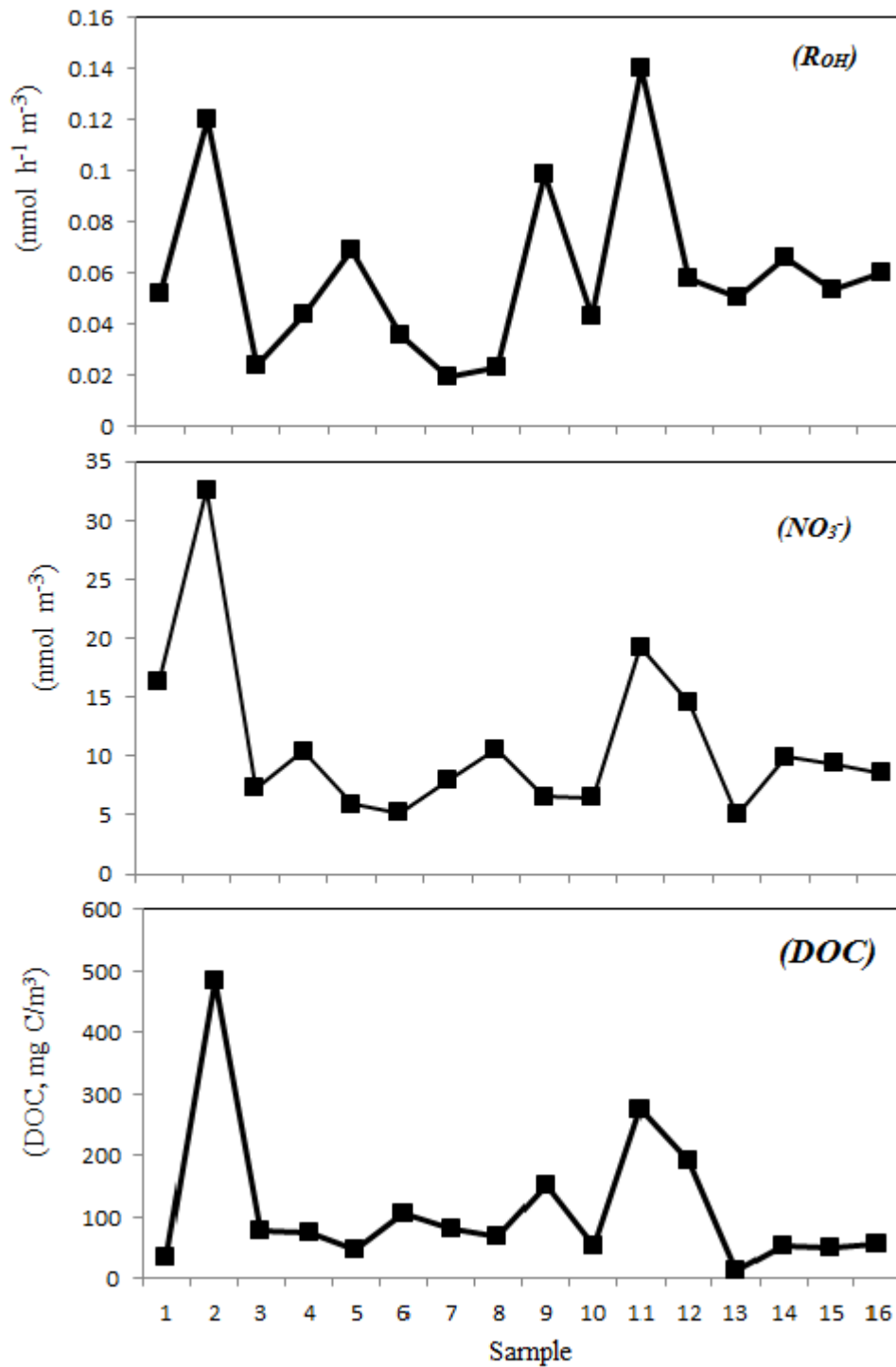
**Figure 3-8.** Variations in the photoformation rates of •OH and concentrations of $NO_3^-$ and DOC in the WEA samples of marine aerosol collected in the Seto Inland Sea
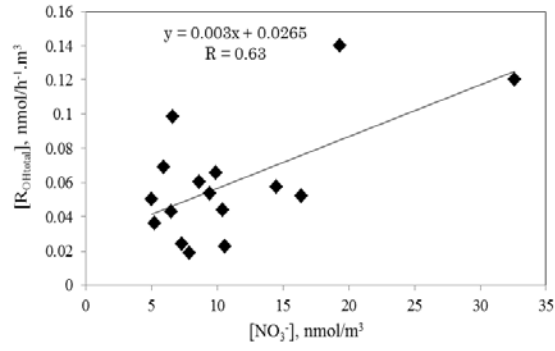
(a)
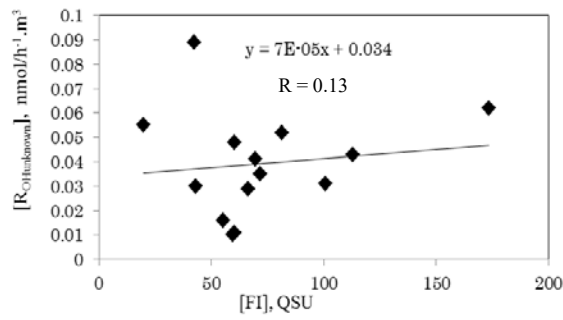


(b)
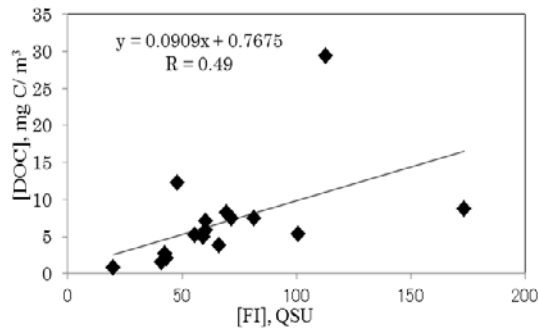


(c)
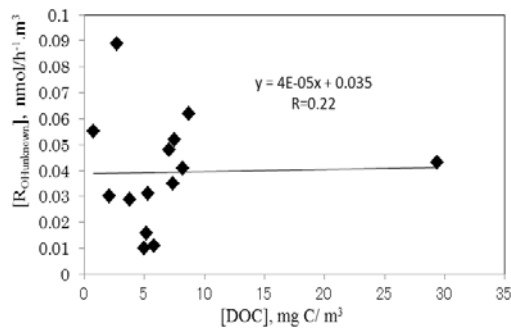


(d)

**Figure 3-9.** Correlation coefficient between: (a) $R_{OHtotal}$ and $[NO_3^-]$ (b) $R_{OHunknown}$ and FI, (c) [DOC] and FI and (d) $R_{OHunknown}$ and [DOC]

**Table 3-8.** Multi-correlation coefficients (R) involving major sources of $^\bullet$OH determined in marine aerosols ($p<0.01$)

| | $R_{OH}$ | $NO_3^-$ | DOC | FI | $R_{OHunk}$ | $FI_A$ | $FI_B$ | $FI_C$ | $NO_2^-$ | $H_2O_2$ |
|---|---|---|---|---|---|---|---|---|---|---|
| $R_{OH}$(nmol h$^{-1}$m$^{-3}$) | 1 | 0.63 | 0.27 | 0.26 | - | 0.20 | 0.12 | 0.06 | - | - |
| $NO_3^-$(nmol m$^{-3}$) | 0.63 | 1 | 0.37 | 0.56 | 0.10 | 0.50 | 0.48 | 0.52 | - | - |
| DOC(mg C m$^{-3}$) | 0.27 | 0.37 | 1 | 0.47 | 0.02 | 0.45 | 0.53 | 0.33 | - | - |
| FI (QSU) | 0.26 | 0.56 | 0.47 | 1 | 0.07 | - | - | - | - | - |
| $R_{OHunk}$(nmol h$^{-1}$m$^{-3}$)[a] | - | 0.10 | 0.02 | 0.07 | 1 | 0.20 | 0.21 | 0.50 | - | - |
| $FI_A$ (QSU) | 0.20 | 0.50 | 0.45 | - | 0.21 | 1 | - | - | - | - |
| $FI_B$ (QSU) | 0.12 | 0.48 | 0.53 | - | 0.21 | - | 1 | - | - | - |
| $FI_C$ (QSU) | 0.06 | 0.52 | 0.33 | - | 0.50 | - | - | 1 | - | - |
| $NO_2^-$(nmol m$^{-3}$) | - | - | - | - | - | - | - | - | 1 | - |
| $H_2O_2$(nmol m$^{-3}$) | - | - | - | - | - | - | - | - | - | 1 |

*Notes:*  [a]$R_{OHunknown} = (R_{OH\ X}\ f_{unknown})/100$     - : *not available*

**Table 3-9.** The contribution of major sources of $^\bullet$OH to the marine aerosols and sea water collected in the Seto Inland Sea, Japan.

| Site | | Contribution[a], % | | | | | |
|---|---|---|---|---|---|---|---|
| | n | $f_{NO3^-}$ | $f_{NO2^-}$ | $f_{H2O2}$ | $f_{photo\text{-}Fenton}$[b] | $f_{Unknown}$[c] | References |
| WEA | 16 | 18.6 | <1 | <1 | 5.1% | 74.3 | *This study* |
| Sea Water | - | <1 | 32 | <1 | - | 66.2 | Takeda *et al.*, 2004 |

*Notes:*  [a]$f_i = [ki[Ci]/R_{OHtotal}] \times 100\ (\%)$     - : *not available*

[b]Generation potential of $^\bullet$OH from photo-Fenton reaction   [c]$f_{unknown} = 100\text{-}(f_{NO3^-}+f_{NO2^-}+f_{H2O2})(\%)$

**Table 3-10.** $R_{OH}$ rate in water-extracts of aerosols

| Site | Light[b] | $R_{OH}$ (nmol.h$^{-1}$.m$^{-3}$) | | | |
| --- | --- | --- | --- | --- | --- |
| | | n | Mean | Range | References |
| Seto Inland Sea, Hiroshima-Japan[a] | Solar | 16 | 0.06 [a] | 0.019-0.14 | *This study* |
| Higashi-Hiroshima, Japan[a] | Solar | 41 | 0.33[a] | 0.02-1.91 | Kondo *et al.*, 2009 |
| Bodega Bay, California, USA | Solar | 1 | 0.092 | -[c] | Anastasio and Newberg, 2007 |
| Alert, Canada | 313 | 2 | 0.010 | 0.008-0.013 | Anastasio and Jordan, 2004 |
| Okinawa, Japan | 313 | 14 | 0.11 | ND-0.21 | Arakaki *et al.*, 2006 |

*Notes :*[a] Normalized to $J_{2-NB} = 0.0093$ s$^{-1}$ [b] Light used to irradiate sample (simulated light) [c] no data
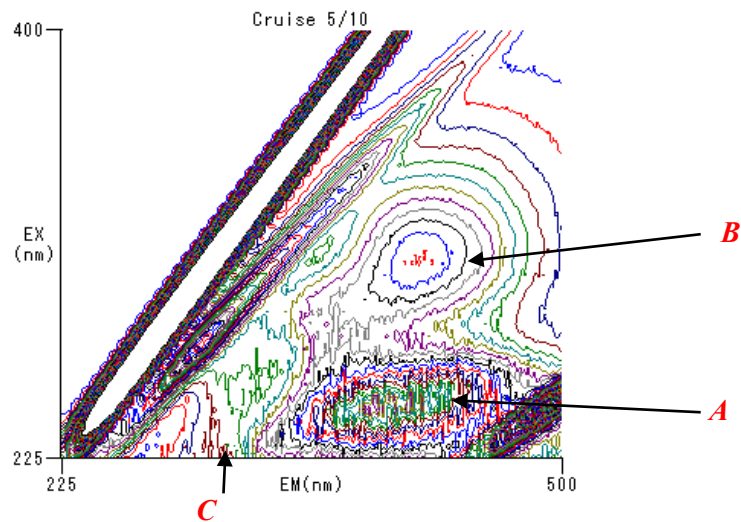
**Figure 3-10.** Contour plots of 3D-EEMs of marine aerosol (sample 5). The spectra were not corrected for Raman and second order light peaks.

**Table 3-11.** Fluorescence intensity (FI) of peaks A, B and C (QSU)

| Sample | A | B | C | FI* |
|---|---|---|---|---|
| 1 | 33.21 | 14.87 | - | 48.08 |
| 2 | 19.85 | - | - | 19.85 |
| 3 | 35.48 | 19.98 | 17.9 | 73.36 |
| 4 | 30.67 | 40.03 | 26.3 | 97 |
| 5 | 107.59 | 65.76 | 49.3 | 222.65 |
| 6 | 42.2 | 24.04 | 22.3 | 88.54 |
| 7 | 38.9 | 20.54 | 24.3 | 83.74 |
| 8 | 37.99 | 22.26 | 22.7 | 82.95 |
| 9 | 30.62 | 11.79 | - | 42.41 |
| 10 | 45.53 | 26.26 | - | 71.79 |
| 11 | 27.37 | 13.8 | 16.3 | 57.47 |
| 12 | 29.4 | 13.88 | 14.4 | 57.68 |
| 13 | 62.86 | 50.07 | 28.2 | 141.13 |
| 14 | 45.81 | 35.58 | 19.4 | 100.79 |
| 15 | 42.46 | 27.08 | 20.1 | 89.64 |
| 16 | 38.51 | 21.71 | 22.1 | 82.32 |
| Mean | 43.65 | 27.18 | 23.61 | 84.96 |
| SD | 19.72 | 16.01 | 8.63 | 46.02 |

*Note:* QSU: Quinine Sulfate Unit    -: not detectable    *FI=A+B+C
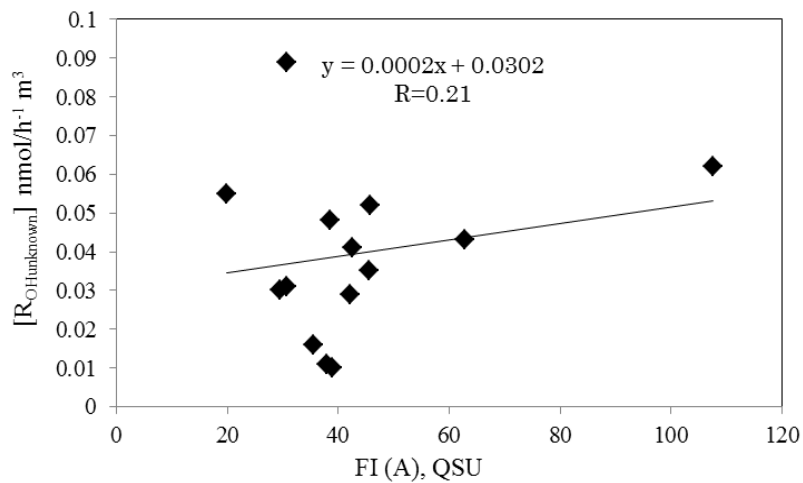
(a)
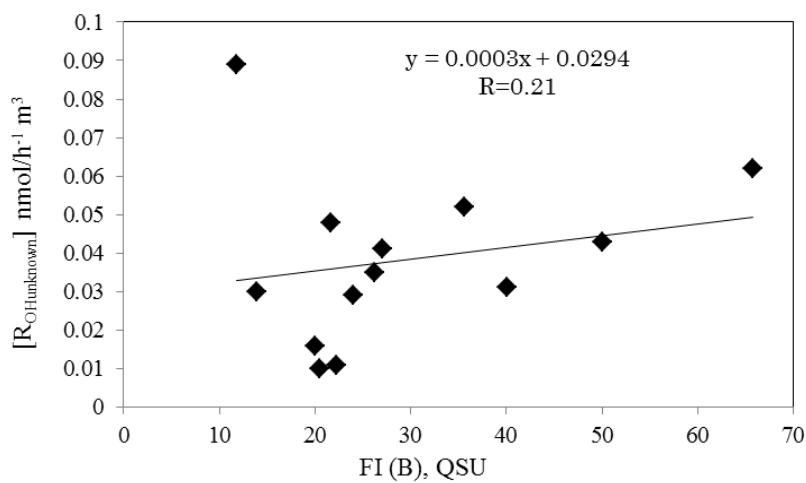


(b)
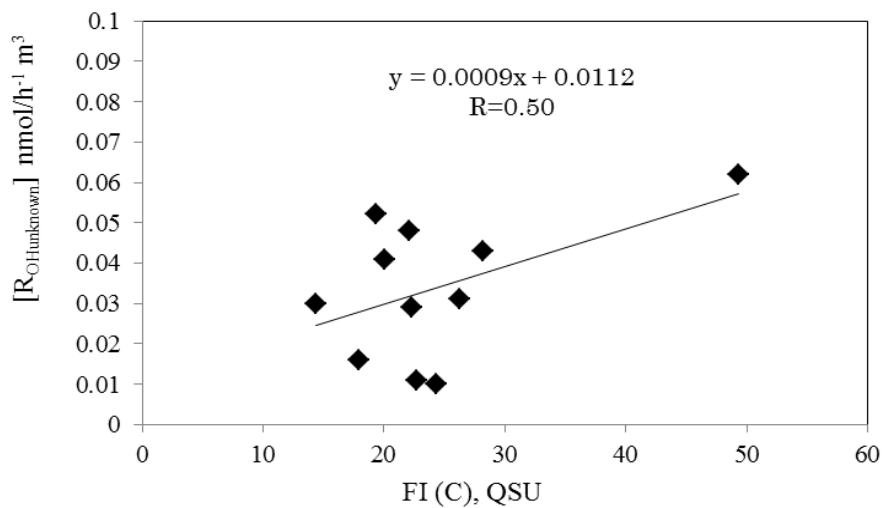


(c)

**Figure 3-11.** Correlation between $R_{OHunknown}$ and fluorescence of peaks A (a), B (b) and C (c).

**Chapter 4**

## Chapter 4

## 4- General Discussion

Photochemical reactions involving the oxidation capacity of  $^\bullet$OH taking place in natural water (river and sea waters) and in the atmospheric condensed phase (cloud, fog, and rain drops, aqueous aerosols and dew) were reported in the past (Mopper and Zhou, 1990; Faust and Hoigné, 1990; Arakaki *et al.*, 1998; Arakaki *et al.*, 2006) (Figure 4-1).

*1990*　　*1992*　　　　*1993*　　　*2004*　　　　　*2008*

| Rain | River water | Cloud and fogwaters | Snowpacks | → | Marine Aerosol |

**Sea water**

*1998*　　　*2001*　　　*2007*

*2004*

*2004*

**Aerosol Particles**

*2011*　　　　　　　　　　*This work*

*2010*

2007

*2006*

**Aqueous solution of water-soluble gases**

*2009*

***This work***
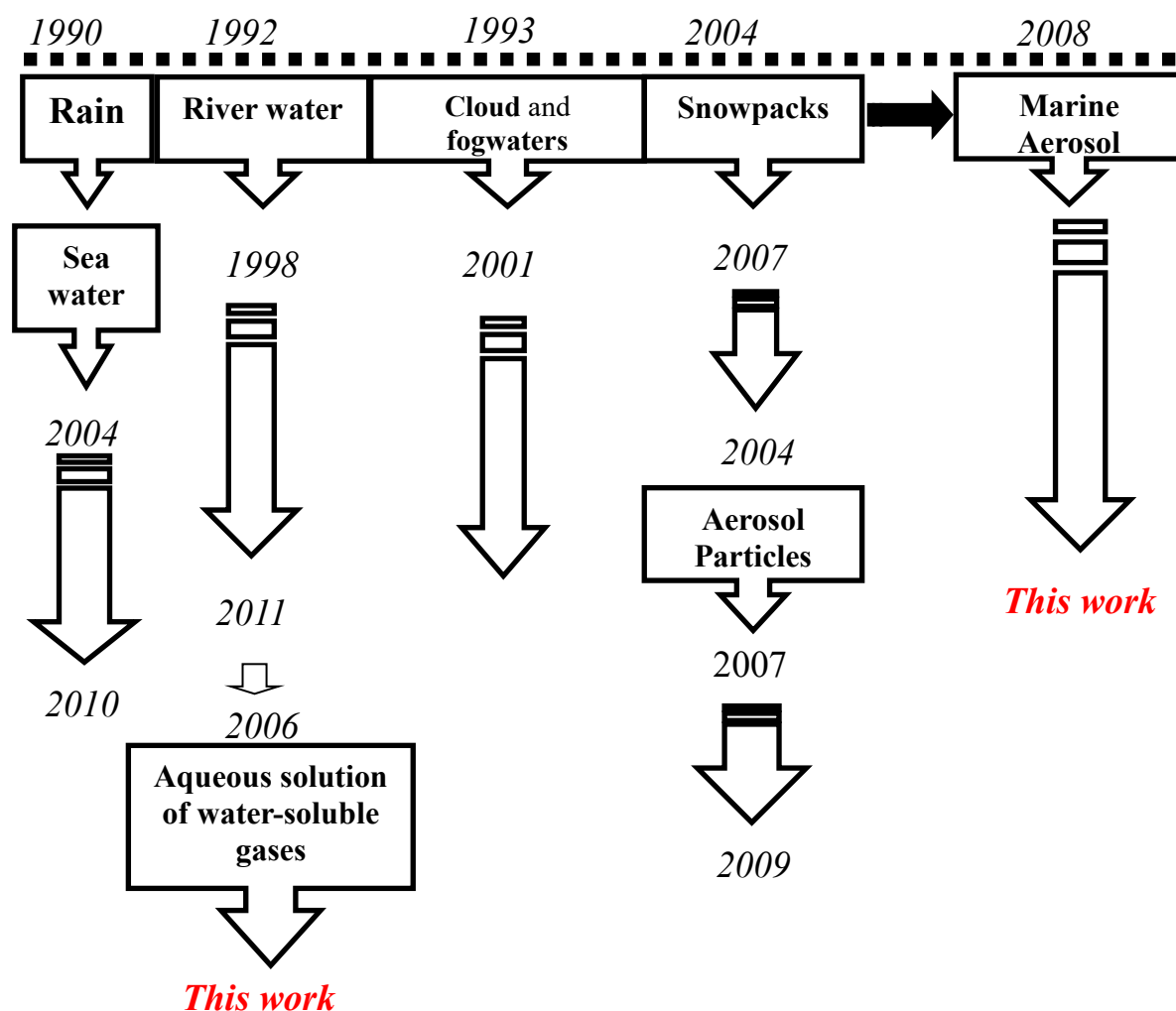
**Figure 4-1.** Previous and recent studies involving •OH generation in aqueous phase

Studies on other natural water such as river and sea water (Nakatani *et al*., 2007; Takeda *et al.*, 2004) help characterize the potential and possible significant sources of  $^\bullet$OH

existing in the atmospheric aqueous-phase (Nakajima *et al.*, 2009). The results point out the photo-Fenton reaction as an important and significant source of $^\bullet OH$ generation. These studies were essential for initiating our present research.

In our study case, we showed the similarities of mechanisms of $^\bullet OH$ photoformation occurring in atmospheric water-extracts of aerosols, aqueous solution of water-soluble gas fraction and natural waters. The results also contributed in clarifying the oxidation capacity of $^\bullet OH$ and identified the main sources from samples collected at different locations. Although the photochemistry of $^\bullet OH$ in the WEA and WSG showed to be the same, the contribution from identified sources of $^\bullet OH$ was observed different and might be related with sampling location.

Our study focused on the $^\bullet OH$ formation from ambient aerosol of Higashi-Hiroshima described in *Chapter 2,* the first findings revealed $^\bullet OH$ generation in atmospheric aqueous solution of water-soluble gas, suggesting the same photochemistry of $^\bullet OH$ production as occurring in atmospheric water-extracts of aerosols. Therefore, the capacity of $^\bullet OH$ formation in the aqueous gas phase may contribute significantly on changing the chemical composition of aerosols.

In addition, the presence of HULIS was suggested as a possible and important source of $^\bullet OH$ generation in aqueous solution of water-soluble gas fraction.

Recent studies detected the presence of HULIS in the atmosphere (Graber and Rudich, 2006; Kondo *et al.*, 2009; Stone *et al.*, 2009; Lin *et al.*, 2010; Ziese *et al.*, 2008) which might causes night-time reaction of Fe (III) converting to Fe (II) and subsequent $^\bullet$OH formation. The results suggested that although HULIS had a relatively small impact on Fe (II) photoformation during the daytime, the night-time formation of Fe(II) in atmospheric condensed phases (e.g., cloud, fog, and rain) by HULIS could be important, and therefore, the "dark" Fenton reaction should also be incorporated into fate models for atmospheric pollutants (Arakaki *et al*, 2010).

More research is required for the aqueous solution of atmospheric water-soluble gas fraction in order to understand the significance of this fraction on the oxidizing capacity of $^\bullet$OH generation involved in the photochemical reactions occurring in the aerosol aqueous phase and its impacts and effect on the environment and human health.

The $^\bullet$OH photochemically generated from the water-extract of marine aerosol of the Seto Inland Sea showed lower photoformation rates than land aerosols. Our results are in agreement with results obtained for the water-extracts of aerosols collected in the coastal and remote locations (Arakaki *et al.*, 2006; Nakajima *et al.*, 2009; Anastasio and Jordan, 2004).

The capacity of $^\bullet OH$ generation determined in the water-extract of marine aerosol particles is useful to estimate the anthropogenic effect through the transport of pollutants from the land to coastal areas.

The results also revealed that among the major sources of $^\bullet OH$, the unknown source was the most important source in the marine aerosol samples as so seawater samples collected in Seto Inland Sea reported by Takeda *et al*, 2004. No clear correlation between the dissolved organic carbon and the fluorescence intensity was found however the presence of 2 major peaks, characteristic of HULIS, leads to discussion about HULIS as the possible and major source of $^\bullet OH$ in marine aerosol.

**4-1- Conclusion**

This study revealed that sources and sinks of $^\bullet OH$ in the WEA fractions from land and marine aerosols are almost same to those of the WSG fractions. In addition, mechanism of $^\bullet OH$ generations occurring in atmospheric aqueous phase, in which HULIS is involved, are probably same/identical to those in natural waters. Therefore, in the analogue of photoformed $^\bullet OH$ in natural waters, $^\bullet OH$ in the WEA and WSG fractions in the atmosphere may significantly control the aqueous phase chemistry, especially degradation rates of several organic matters.

## 4-2- Suggestions for further research

The results presented in this thesis showed the significant percentage of contribution from unknown sources on $^\bullet$OH photoproduction. Further investigations is needed for a better comprehension of the oxidation capacity of the $^\bullet$OH generation in the atmospheric aqueous solution of water-soluble gases and the relationship with dissolved organic compounds found in the unknown sources. In addition, research focused on identification of the organic water-soluble fraction, characterization of the organic compounds present and $^\bullet$OH photogeneration mechanisms are important. Optical properties and absorbance may be related with seasons, e.g., summer and winter, would be an important factor to elucidate the origin of the HULIS in the aqueous aerosol environment.

# References

Anastasio, C. and Jordan, A.L, 2004. Photoformation of hydroxyl radical and peroxide in aerosol particles from Alert, Nunavut: implications for aerosol and snowpack chemistry in the Artic. Atmospheric Environment 38, 1153-1166.

Arakaki, T., Miyake, T., Shibata, M. and Sakugawa, H., 1998. Measurement of photochemically formed hydroxyl radical in rain and dew waters. The Chemical Society of Japan, 9, 619-625 (in Japanese).

Arakaki, T., Kuroki, Y., Okada, K., Nakama, Y., Ikota, H., Higuchi, T., Uehara, M., Tanahara, A., 2006. Chemical composition of photochemical formation of hydroxyl radical in aqueous extracts of aerosol particles collected in Okinawa, Japan. Atmospheric Environment 40, 4764-4774.

Arakaki, T., Saito, K., Okada, K., Nakajima, H., Hitomi, Y., 2010. Contribution of fulvic acid to the photochemical formation of Fe (II) in acidic Suwannee River fulvic acid solutions. Chemosphere 78, 1023-1027.

Faust, B.C. and Hoigné, J., 1990. Photolysis of Fe (III)-hydroxyl complexes as sources of OH radicals in clouds, fog and rain. Atmospheric Environment 24A (1), 79-89.

Graber, E. R. and Rudich, Y., 2006. Atmospheric HULIS: How humic-like are they? A comprehensive and critical review. Atmospheric Chemistry and Physics 6, 729-753.

Kondo, H., Chiwa, M., Sakugawa, H., 2009. Photochemical formation and scavenging mechanisms of hydroxyl radical in water-extracts of atmospheric aerosol collected in Higashi-Hiroshima, Japan. Geochemistry 43, 15-25 (in Japanese).

Lin, P., Huang, X., He, L., Yu, J.Z., 2010. Abundance and size distribution of HULIS in ambient aerosols at a rural site in South China. Journal of Aerosol Science 41, 74-87.

Mopper, K. and Zhou, X., 1990. Hydroxyl radical photoproduction in the Sea and its potential impact on marine processes. Science 250, 661-664.

Nakajima, H., Okada, K., Kuroki, Y., Nakama, Y., Handa, D., Arakaki, T., Tanahara, A., 2008. Photochemical formation of peroxides and fluorescence characteristics of the water-soluble fraction of bulk aerosols collected in Okinawa, Japan. Atmospheric Environment 42, 3046-3058.

Nakatani, N., Ueda, M., Shindo, H., Takeda, K., and Sakugawa, H. 2007. Contribution of the photo-Fenton reaction to hydroxyl radical formation rates in river and rain water samples. Analytical Sciences, 23, 1137-1142.

Takeda, K., Tadedoi, H., Yamaji, S., Ohta, K., Sakugawa, H., 2004. Determination of hydroxyl radical photoproduction rates in natural waters. Analytical Sciences 20, 153-159.

Stone,E. A., Hedman, C. J.,R. J. Sheesley, Shafer, M.M., Schauer, J.J., 2009. Investigating the chemical nature of humic-like substances (HULIS) in North American atmospheric aerosols by liquid chromatography tandem mass. Atmospheric Environment 43, 4205-4213.

Ziese, M., Wex, H., Nilsson, E., Salma, I., Ocskay, R., Henning, T., Massling, A. and Stratmann, F., 2008. Hygroscopic growth and activation of HULIS particles: experimental data and a new interactive parameterization scheme for complex aerosol particles. Atmospheric Chemistry and Physics 8, 1855-1866.

# Acknowledgements

*"I was taught that the way of progress is neither swift nor easy."*

**Marie Curie**